ACR No. L5G18

NATIONAL ADVISORY COMMITTEE FOR AERONAUTICS

WARTIME REPORT

ORIGINALLY ISSUED
October 1945 as
Advance [redacted] Report L5G18

DATA FOR DESIGN OF ENTRANCE VANES FROM TWO-DIMENSIONAL TESTS OF AIRFOILS IN CASCADE

By Charles M. Zimmey and Viola M. Lappi

Langley Memorial Aeronautical Laboratory
Langley Field, Va.

WASHINGTON

NACA ACR No. L5G18

NATIONAL ADVISORY COMMITTEE FOR AERONAUTICS

ADVANCE [redacted] REPORT

DATA FOR DESIGN OF ENTRANCE VANES FROM TWO-DIMENSIONAL TESTS OF AIRFOILS IN CASCADE

By Charles M. Zimney and Viola M. Lappi

SUMMARY

As a part of a program of the NACA directed toward increasing the efficiency of compressors and turbines, data were obtained for application to the design of entrance vanes for axfax-flow compressors or turbines. A series of blower-blade sections with relatively high critical speeds have been developed for turning air efficiently from 0° to 80° starting with an axial direction. Tests were made of five NACA 65.-series blower blades (modified NACA 65(216)-010 airfoils) and of four experimentally designed blower blades in a stationary cascade at low Mach numbers. The turning effectiveness and the pressure distributions of these blade sections at various angles of attack were evaluated over a range of solidities near 1. '%.trance-vane design charts are presented that give a blade section end angle of attack for any desired turning angle, The Glades thus obtained operate with peak-free pressure distributions. Approximate critical Mach numbers were calculated from the pressure distributions.

INTRODUCTION

Previous investigations of airfoils in a cascade (reference 1) have attempted to simulate flow conditions through a rotor or a stator involving a pressure rise, The present investigation has been made to provide information concerning the flow through entrance vanes involving a pressure drop. A pressure rise' from the leading edge to the trailing edge is accompanied by a reduction of velocity relative to the blades, whereas a pressure drop is accompanied by an increase in velocity relative to the blades. The object of entrance-vane

design is to turn the initial air through a specified angle with a minimum of losses. It seems likely that critical speeds could be increased and boundary-layer losses decreased by eliminating velocity peaks; tests were consequently made for two series of blades to obtain a range of turning angle for a given blade section while maintaining a pressure distribution without peaks. The tests were made in a two-dimensional low-speed cascade tunnel at the Langley Memorial Aeronautical Laboratory and are a part of the NACA program to increase the efficiency of compressors and turbines. The purpose of the investigation was to develop efficient blades operating at 0° stagger that would turn the air through angles from 0° to 80°.

SYMBOLS

a	angle of attack, the angle between the initial air and the chord line of the blower blade
α_d	design angle of attack of blower blade in cascade
q	local dynamic pressure
q_1	dynamic pressure of initial air
q_2	dynamic pressure of air behind the blades
q_o	mean dynamic pressure $\left(\frac{q_1 + q_2 + 2\sqrt{q_1 q_2}\cos\theta}{4}\right)$
V_1	velocity of initial air
V_2	velocity of air behind the blades
V_o	mean velocity of air $\left(\frac{1}{2}\text{ vector sum of } V_1 \text{ and } V_2\right)$
ΔV	vector difference of velocities $(V_1 - V_2)$
p_1	initial static pressure
p_2	static pressure behind the blades, equal to atmospheric pressure
p_{2t}	theoretical static pressure behind the blades

[redacted]

Δp pressure drop across cascade $(p_2 - p_1)$

σ solidity, ratio of chord to gap

θ angle through which air is turned by blades

c chord

c_{l_d} theoretical design lift coefficient of blade in free air

β stagger, angle between perpendicular to cascade and entering air

M_{cr} critical Mach number, stream Mach number at which the velocity of sound is reached on the blade

A_1 cross-sectional area of initial air stream

A_2 area of air stream behind blades

x chordwise distance from leading edge

y vertical distance from chord

APPARATUS AND TEST PROCEDURE

The two-dimensional low-speed cascade tunnel described in reference 1 has been rebuilt to permit variation of the stagger angle and also of the solidity. This change was made possible by constructing walls with removable circular plates that could be rotated. For the present tests, the cascade tunnel was further modified by eliminating the boundary-layer control system on the walls; however, small gaps, which served as boundary-layer slots on the floors, were left between the top and bottom blades of the cascade and the floors. A vertical cross section of the apparatus is schematically shown in figure 1.

Two families of blower blades were investigated. For low turning angles, the NACA 65-series blower-blade sections were used, whereas for turning angles greater than 30° a series of experimentally derived blower blades was used. The NACA 65-series blower-blade sections (NACA

[redacted]

65(216)-010 airfoils with a thickened trailing edge) cambered for lift coefficients of 0.1, 0.2, 0.4, 0.8, and 1.2 were tested at solidities of 0.88, 1.00, and 1.50. These theoretical design lift coefficients are for isolated profiles in free air. The method of obtaining the ordinates of blade sections with the same basic thickness and varying cambers is given in reference 2. The ordinates for the blade sections tested are given in tables I to V. Cross sections of these blades are shown in figure 2. In order to conform with previous work (reference 1), a chord of 5 inches was used. The span, however, was increased to $5\frac{1}{2}$ inches because of the slightly different tunnel setup. A cascade of five blower blades was used in all the tests.

Mean lines that gave higher turning angles with peak-free pressure distributions were experimentally derived. Cascade tests of flexible plates at solidities of approximately 0.9 and 1.4 were used to determine mean-line shapes. These plates were altered in shape until a pressure distribution without peaks was obtained. From these tests, four shapes (fig. 3) were selected as mean lines for blades to cover a range of turning angle from 30° to 80°. The ordinates for these mean lines (designated A, B, C, and D) are given in table VI. Blade sections were designed by combining a basic thickness with the various mean lines (fig. 4). The basic thickness for the NACA 64(215)-006 airfoil section with a thickened trailing edge was used. This section was chosen rather than the NACA 65-series blower-blade section because the NACA 65-series section gave three points of reversed curvature on the lower surface. By combining the thickness with a mean line according to the conventional method (reference 2), a very sharp leading edge was obtained; hence, the mean line rather than the chord was divided into the NACA standard stations and the basic thickness was applied perpendicular to the mean line at these points. The ordinates for the derived sections, which were tested at solidities of approximately 0.95 and 1.40, are given in tables VII to X.

It was assumed that the initial air-flow direction was parallel to the tunnel walls. The total and static pressures were measured by total-head tubes on the floor and ceiling of the tunnel and a row of wall static-pressure

orifices located $\frac{1}{2}$ chord length ahead of the blades (fig. 1). In all tests the central blade was equipped with pressure-distribution orifices.

The angle through which the air was turned by the blades was measured approximately $\frac{1}{2}$ chord length behind the blades. Measurements were made with a cylindrical yaw tube provided with a fixed arm. The tube was $\frac{1}{4}$ inch in diameter with two static-pressure orifices at an included angle of 80°. The angle of the arm with respect to the air, when both tubes read equal pressures, was found by calibration. The "null" method of taking measurements was used; that is, the arm was adjusted so that the tubes to which the two orifices were connected read the same and then the angle at which the arm was set was found with an inclinometer (an angle measuring device). An average turning angle was obtained by surveying the gaps adjacent to the central blade. The experimental accuracy of the turning angles was $\pm\frac{1}{2}^\circ$ for turning angles up to about 60° and decreased to $\pm 1\frac{1}{2}^\circ$ for angles from about 60° to 80°. These tests were conducted over a range of Reynolds numbers from 185,000 to 350,000.

RESULTS AND DISCUSSION

The blade characteristics are based on "mean air" conditions as in reference 1. The mean velocity V_o (fig. 5(a)) is therefore used as a basis for determining the mean dynamic pressure q_o. The pressure distributions for the different blower blades at various angles of attack for each solidity are shown in figures 6 to 27. The quantity plotted is the local dynamic pressure q divided by q_o. The accuracy of these results was impaired by the thick boundary layer along the walls and the difficulty of measuring the entrance velocity for the high turning angles. The boundary layer, which was at times $\frac{1}{2}$ inch thick, was due to the length of the tunnel walls ahead

[redacted]

of the blades and the interference of the blade attachments. High angles of attack throttled the tunnel; hence, the velocity of the air ahead of the cascade was reduced considerably. Since the absolute error of pressure measurements is constant, a considerable reduction in measured initial dynamic pressure magnifies the error in determining the mean dynamic pressure. The tests, therefore, do not give the actual pressures on the blades accurately but the results may be used to select pressure distributions without peaks.

The theoretical pressure change due to a cascade of blades, if no energy losses and incompressible flow are assumed, can be calculated from the following equation (reference 1) provided the turning angle is known:

$$\frac{\Delta p}{q_1} = 1 - \left[\frac{\cos \quad}{\cos (\quad - \theta)}\right]^2$$

For $\beta = 0^\circ$ (fig. 5(b)),

$$\frac{\Delta p}{q_1} = 1 - \frac{1}{\cos^2\theta}$$

In figure 28, the theoretical pressure drop $\Delta p/q_1$ for various turning angles is shown.

It may be noted that in the case of the experimentally derived blower blades for high turning angles (figs. 26 and 27) the theoretical static pressure behind the blades p_{2_t} and the measured static pressure behind the blades p_2 show a very large discrepancy. These values of static pressures are shown in terms of q/q_o in figures 6 to 27. The theoretical static pressure was found by adding the theoretical pressure drop to the initial static pressure p_1. The deviation was caused by throttling of the tunnel and the characteristics of the equation used to calculate $\Delta p/q_1$. A very small discrepancy in the large turning angles gave a very large change in the calculated pressure drop. (See fig. 28.)

For each blade section, the range of angle of attack that gave pressure distributions without undesirable peaks was found. In the case of the NACA 65-series blades, the angle of attack that gave the maximum turning angle with a flat pressure distribution was selected as the design condition for a given solidity. This angle is labeled as design angle of attack in figures 9 to 20. For the experimentally designed sections, a range of design angle of attack was selected from the desirable pressure distributions at the higher solidities (figs. 22, 24, 26, and 27). These two series of blower-blade sections, with relatively high critical speeds, will efficiently turn air flowing in an axial direction from 0° to 80°.

It is seen from the pressure distributions at the lower solidities (figs. 21, 23, and 25) that the exit velocities are very much lower than the maximum local velocities on the top surface. These blade sections are therefore not recommended for installations in which high exit Mach numbers are encountered. The turning angles for various angles of attack are shown in figures 29 to 32 and the turning angles not recommended are indicated by dashed lines. Within the range of solidities tested, the cascade of blades shows characteristics of the infinite solidity case $\frac{d\theta}{d\alpha} \approx 1$.

The data of the NACA 65-series blades indicate that for low design cambers ($c_{l_d} = 0.1$ and 0.2), the design angle of attack depends little, if any, upon solidity for the range of solidity covered in the present tests. For the higher-cambered sections ($c_{l_d} = 0.4$, 0.8, and 1.2), the angle of attack for optimum operation is essentially independent of solidity for the range from 0.88 to 1.00 but with an increase of solidity to 1.50 the optimum operating angle is increased. These results are expected because for low cambers an increase in solidity produces little change of turning angle and, therefore, the direction of mean flow is changed only slightly. For high cambers, an increase of solidity increases the turning angle appreciably. This increased turning angle changes the mean flow so as to decrease the angle of attack of the blades relative to the mean flow; thus, for the high-camber blades, the angle of attack for optimum operation must be increased with an increase of solidity.

[redacted]

At the low solidity of 0.88, the data indicate that the change of turning angle with angle of attack is greater for the NACA 65-(12)10 blade than for the lower-cambered blades in this series. The reason for this difference is not known, although this high-camber blade may actually be more efficient at the solidity of 0.88 or the difference may be due to experimental error.

The NACA 65-110 blades have pressure peaks on the nose for all angles of attack; therefore, the use of these blades for high Mach numbers would not be desirable. The angle-of-attack range that is covered by pressure distributions without peaks of the NACA 65-210 blade, however, overlaps sufficiently to cover the turning angle corresponding to the design-angle-of-attack range of the NACA 65-110 blade.

Examination of the pressure distributions of the experimentally designed blades shows that the blades operated through a wide range of angle of attack with peak-free pressure distributions. The flat plates used to derive the mean-line shapes of these blades had a very narrow operating range because of the sharp leading edge.

Approximate critical Mach numbers (table XI) were obtained by use of the von Kármán-Tsien equations (reference 3). The value of q/q_o for calculating the critical Mach number was taken from the pressure distributions for α_d or the highest velocity point in the design range. When no α_d or range is indicated, the value of q/q_o was selected from a peak-free pressure distribution. The value of q/q_o, in each case, was chosen from either the peak value of the pressure distributions or the theoretical value at the trailing edge depending on which was the larger. Interference effects made it impossible to estimate the critical Mach number to the same degree of accuracy as is now possible for isolated airfoils but an approximation to the critical speed can be made. It appears from these approximate calculations that the critical Mach number tends to be independent of the solidity. As may be expected, the blades with low turning angles had a higher critical Mach number than the blades with high turning angles.

APPLICATION OF RESULTS TO ENTRANCE-VANE DESIGN

The data obtained are presented in figures 32 and 33 in forms intended to permit turbine and compressor designers readily to select entrance vanes (entering air assumed to be flowing axially) for a specific machine. Two distinct design procedures are presented. First, in the case of the lower turning angles ($<30^\circ$), the NACA 65-series blower-blade sections can be recommended. The camber and angle of attack to be used to obtain a specified turning angle with a peak-free pressure distribution can be found from figure 33. This design chart does not contain data for turning angles less than about 4°, but these angles can be obtained directly from the turning angle and pressure-distribution charts. The application of the design chart may be illustrated as follows: Suppose it is desired to turn air flowing in an axial direction 20° by use of a row of blades with a solidity of 1.35. Reference to figure 33 shows that a blower blade cambered for a lift coefficient of 0.85 is indicated and that it should be operated at an angle of attack of 13.5°. The method of designing such a blade is given in reference 2. If some choice is available in the solidity to be used, it is possible to avoid computations by adjusting the solidity until figure 33 indicates that a blower blade of standard camber could be used.

In order to design entrance vanes for turning air through angles greater than 30°, figure 32 can be used. Four entrance-vane sections have been developed that, if used at the appropriate solidity and angle of attack, cover the turning-angle range of 30° to 80°. The solid lines represent regions in which these blades have peak-free pressure distributions; thus, for example, if it is desired to turn air efficiently through 52°, it could be done either with a cascade of NACA 64-(C)06 blade sections at an angle of attack of 32.3° and a solidity of 1.40 or with a cascade of NACA 64-(E)06 blade sections at an angle of attack of 38.1° and a solidity of 1.435.

CONCLUSIONS

Data have been obtained from tests made on five NACA 65-series blower-blade sections and four experimentally derived blower-blade sections and are presented

[redacted]

in the form of design charts for entrance vanes for axial-flow compressors or turbines. These design charts give a blade section and angle of attack for any desired turning angle. The blades thus obtained operate with peak-free pressure distributions. These two series of blower-blade sections, with relatively high critical speeds, will efficiently turn air flowing in an axial direction from 0° to 80°.

Langley Memorial Aeronautical Laboratory
National Advisory Committee for Aeronautics
Langley Field, Va.

REFERENCES

1. Kantrowitz, Arthur, and Daum, Fred L.: Preliminary Experimental Investigation of Airfoils in Cascade. NACA CB, July 1942.

2. Jacobs, Eastman N., Ward, Kenneth E., and Pinkerton, Robert M.: The Characteristics of 78 Related Airfoil Sections from Tests in the Variable-Density Wind Tunnel. NACA Rep. No. 460, 1933.

3. von Kármán, Th.: Compressibility Effects in Aerodynamics. Jour. Aero. Sci., vol. 8, no. 9, July 1941, pp. 337-356.

[redacted]

TABLE I

ORDINATES FOR NACA 65-110 BLOWER BLADE

[Derived from NACA 65(216)-110 airfoil combined with y = 0.0015x; stations and ordinates in percent of chord]

Upper surface		Lower surface	
x	y	x	y
0	0	0	0
.468	.776	.532	-.726
.715	.924	.785	-.854
1.211	1.177	1.289	-1.069
2.454	1.663	2.546	-1.477
4.948	2.379	5.052	-2.063
7.446	2.920	7.554	-2.496
9.946	3.369	10.054	-2.1353
14.948	4.082	15.052	-3.410
19.953	4.616	20.047	-3.820
24.960	5.018	25.040	-4.122
29.967	5.310	30.033	-4.338
34.975	5.497	35.025	-4.467
39.984	5.593	40.016	-4.521
44.992	5.577	45.008	-4.481
50.000	5.422	50.000	-4.318
55.007	5.118	54.993	-4.G22
60.013	4.687	59.987	-3.615
65.018	4.142	64.982	-3.112
70.020	3.524	69.980	-2.552
75.021	2.899	74.979	-2.003
80.020	2.245	79.980	-1.449
85.017	1.587	84.983	-.915
90.013	1.007	89.987	-.491
95.008	.512	94.992	-.196
100.006	.150	99.994	-.150
L.E. radius: 0.666			

NATIONAL ADVISORY
COMMITTEE FOR AERONAUTICS

[redacted]

TABLE II

ORDINATES FOR NACA 65-210 BLOWER BLADE

[Derived from NACA 65(216)-210 airfoil combined with y = 0.0015x; stations and ordinates in percent of chord]

Upper surface		Lower surface	
x	y	x	y
0	0	0	0
.437	.799	.563	-.699
.681	.957	.319	-.817
1.172	1.228	1.328	-1.014
2.409	1.754	2.591	-1.382
4.896	2.536	5.104	-1.904
7.392	3.131	7.608	-2.283
9.891	3.626	10.109	-2.592
14.897	4.418	15.103	-3.072
19.907	5.013	20.093	-3.421
24.920	5.464	25.080	-3.674
29.935	5.796	30.065	-3.852
34.951	6.012	35.049	-3.952
39.967	6.128	40.033	-3.986
44.984	6.124	45.016	-3.934
50.000	5.973	50.000	-3.767
55.015	5.665	54.985	-3.475
60.027	5.222	59.973	-3.080
65.036	4.657	64.964	-2.597
70.041	4.010	69.959	-2.066
75.043	3.346	74.957	-1.556
80.041	2.643	79.959	-1.051
85.035	1.924	84.965	-.578
90.026	1.266	89.974	-.239
95.017	.670	94.983	-.038
100.013	.149	99.987	-.149
L.E. radius: 0.666			

NATIONAL ADVISORY
COMMITTEE FOR AERONAUTICS

[redacted]

TABLE III

ORDINATES FOR NACA 65-410 BLOWER BLADE

[Derived from NACA 65(216)-410 airfoil combined with y = 0.0015x; stations and ordinates in percent of chord]

Upper surface		Lower surface	
x	y	x	y
0	0	0	0
.375	.842	.625	-.642
.613	1.020	.887	-.740
1.095	1.327	1.405	-.899
2.318	1.932	2.682	-1.188
4.793	2.844	5.207	-1.580
7.284	3.548	7.716	-1.852
9.783	4.137	10.217	-2.069
14.793	5.086	15.207	-2.394
19.814	5.806	20.186	-2.622
24.840	6.357	25.160	-2.777
29.870	6.765	30.130	-2.877
34.902	7.044	35.098	-2.924
39.935	7.199	40.065	-2.915
44.968	7.219	45.032	-2.839
50.000	7.076	50.000	-2.664
55.029	6.762	54.971	-2.382
60.054	6.291	59.946	-2.007
65.071	5.686	64.929	-1.566
70.082	4.994	69.918	-1.106
75.086	4.238	74.914	-.658
80.081	3.434	79.919	-.250
85.070	2.607	84.930	.085
90.052	1.781	89.948	.287
95.033	.985	94.967	.279
100.033	.146	99.967	-.146
L.E. radius: 0.666			

NATIONAL ADVISORY
COMMITTEE FOR AERONAUTICS

[redacted]

TABLE IV

ORDINATES FOR NACA 65-810 BLOWER BLADE

[Derived from NACA 65(216)-810 airfoil combined with y = 0.0015x; stations and ordinates in percent of chord]

Upper surface		Lower surface	
x	y	x	y
0	0	0	0
.260	.913	.740	-.513
.486	1.130	1.014	-.570
.949	1.510	1.551	-.654
2.143	2.274	2.857	-.786
4.591	3.448	5.409	-.920
7.072	4.371	7.928	-.979
9.569	5.149	10.431	-1,013
14.589	6.415	15.411	-1.031
19.629	7.386	20.371	-1.018
24.681	8.139	25.319	-.979
29.740	8.705	30.260	-.929
34.804	9.093	35.196	-.858
39.870	9.339	43.130	-.771
44.936	9.409	45.064	-.649
50.000	9.282	50.000	-.458
55.058	8.950	54.942	-.190
60.107	8.434	59.893	.134
65.143	7.744	64.E57	.496
70.164	6.922	69.836	.854
75.171	6.025	74.823	1.135
80.162	5.024	79.838	1.344
85.137	3.935	84.E63	1.449
90.104	2.810	89.E96	1.326
95.065	1.612	94.935	.916
100.048	.142	99.952	-.142

L.E. radius: 0.666

NATIONAL ADVISORY
COMMITTEE FOR AERONAUTICS

[redacted]

TABLE V

ORDINATES FOR NACA 65-(12)10 BLOWER BLADE

[Derived from NACA 65(216)-(12)10 airfoil combined with $y = 0.0015x$; stations and ordinates in percent of chord]

Upper surface		Lower surface	
x	y	x	y
0	0	0	0
.161	.971	.839	-.371
.374	1.227	1.126	-.387
.817	1.679	1.683	-.395
1.981	2.599	3.019	-.367
4.399	4.035	5.601	-.243
6.868	5.178	8.132	-.090
9.361	6.147	10.639	.057
14.388	7.734	15.612	.342
19.477	8.958	20.553	.594
24.523	9.915	25.477	.825
29.611	10.640	30.389	1.024
34.706	11.153	35.294	1.207
39.804	11.479	40.196	1.373
44.904	11.598	45.096	1.542
50.000	11.488	50.000	1.748
55.087	11.139	54.913	2.001
60.161	10.574	59.839	2.278
65.214	9.801	64.786	2.559
70.245	8.860	69.755	2.804
75.256	7.808	74.744	2.932
80.242	6.607	79.758	2.945
85.204	5.272	84.796	2.804
90.154	3.835	89.846	2.389
95.096	2.237	94.904	1.555
100.068	.134	99.932	-.134
L.E. radius: 0.666			

NATIONAL ADVISORY
COMMITTEE FOR AERONAUTICS

[redacted]

TABLE VI

EXPERIMENTALLY DERIVED MEAN LINES

[Stations and ordinates in percent of chord]

x	A	E	C	D
0	0	0	0	0
.5	.44	.58	.65	5.00
.75	.66	.83	.94	5.69
1.25	1.07	1.38	1.55	6.75
2.5	2.01	2.59	2.98	8.73
5.0	3.55	4.56	5.48	11.34
7.5	4.74	6.02	7.50	13.10
10	5.68	7.16	9.12	14.38
15	7.03	8.82	11.51	16.15
20	7.95	9.98	13.20	17.21
25	8.50	10.90	14.39	17.76
30	8.82	11.55	15.14	17.85
35	9.12	11.95	15.50	17.57
40	9.23	12.10	15.56	16.97
45	9.35	12.06	15.38	16.16
50	9.33	11.88	15.02	15.23
55	9.20	11.42	14.49	14.16
60	8.86	10.75	13.78	12.93
65	8.34	9.83	12.73	11.64
70	7.64	8.71	11.38	10.33
75	6.70	7.57	9.78	8.96
80	5.58	6.37	8.00	7.41
85	4.35	5.01	6.01	5.74
90	3.00	3.49	4.04	3.86
95	1.56	1.80	2.02	1.94
100	0	0	0	0

NATIONAL ADVISORY
COMMITTEE FOR AERONAUTICS

[redacted]

TABLE VII

ORDINATES FOR NACA 64-(A)06 BLOWER BLADE

[Stations and ordinates in percent of chord]

Upper surface		Lower surface	
x	y	x	y
0	0.57	0	0
.5	1.40	.5	-.09
.75	1.72	.75	-.02
1.25	2.33	1.25	.17
2.5	3.55	2.5	.77
5.0	5.43	5.0	1.86
7.5	6.84	7.5	2.78
10	7.97	10	3.51
15	9.60	15	4.54
20	10.73	20	5.18
25	11.46	25	5.56
30	11.90	30	5.79
35	12.22	35	6.01
40	12.37	40	6.13
45	12.34	45	6.34
50	12.17	50	6.49
55	11.82	55	6.56
60	11.25	60	6.48
65	10.47	65	6.24
70	9.44	70	5.84
75	8.19	75	5.22
80	6.74	80	4.44
85	5.17	85	3.53
90	3.52	90	2.50
95	1.82	95	1.25
100	.14	100	-.18
L.E. radius: 0.269			

NATIONAL ADVISORY
COMMITTEE FOR AERONAUTICS

[redacted]

TABLE VIII

ORDINATES FOR NACA 64-(B)06 BLOWER BLADE

[Stations and ordinates in percent of chord)

Upper surface		Lower surface	
x	Y	x	Y
0	0.79	0	0
.5	1.82	.5	-.02
.75	2.24	.75	.07
1.25	2.97	1.25	.35
2.E	4.48	2.5	1.14
5.0	6.66	5.0	2.66
7.5	8.29	7.5	3.88
10	3.58	10	4.82
15	11.51	15	6.18
20	12.90	20	7.13
25	13.95	25	7.86
30	14.70	30	8.40
35	15.12	35	8.75
40	15.26	40	8.93
45	15.16	45	8.98
50	14.77	50	8.93
55	14.12	55	8.71
60	23.21	60	8.29
65	12.03	65	7.63
70	10.63	70	6.83
75	5.14	75	6.01
80	'7.61	80	5.14
85	5.91	E5	4.12
90	4.0a	90	2.88
95	2.13	95	1.44
100	.1.6	100	-.19

L.E. radius: 0.274

NATIONAL ADVISORY
COMMITTEE FOR AERONAUTICS

[redacted]

TABLE IX

ORDINATES FOR NACA 64-(C)06 BLOWER BLADE

[Stations and ordinates in percent of chord]

Upper surface		Lower surface	
x	y	x	y
0	1.00	0	0
.5	2.09	.5	0
.75	2.54	.75	.12
1.25	3.38	1.25	.42
2.50	5.19	2.50	1.31
5.00	8.03	5.00	3.27
7.50	10.19	7.50	5.05
10	11.84	10	6.50
15	14.40	15	8.67
20	16.30	20	10.18
25	17.58	25	11.24
30	18.37	30	11.90
35	18.77	35	12.23
40	18.83	40	12.32
45	18.56	45	12.22
50	18.02	50	12.02
55	17.30	55	11.72
60	16.33	60	11.20
65	15.03	65	10.40
70	13.40	70	9.40
75	11.49	75	8.16
80	9.35	80	6.71
85	7.01	85	5.10
90	4.67	90	3.40
95	2.37	95	1.66
100	.16	100	-.11

L.E. radius: 0.281

NATIONAL ADVISORY
COMMITTEE FOR AERONAUTICS

[redacted]

TABLE X

ORDINATES FOR NACA 64-(D)06 BLOWER BLADE

[Stations and ordinates in percent of chord]

Upper surface		Lower surface	
x	Y	x	y
-1.00	5.08	-1.00	2.28
-.75	6.35	-.75	1.12
-.50	7.22	-.50	.43
0	8.38	0	0
.50	9.25	.50	.50
.75	9.66	.75	1.12
1.25	10.42	1.25	2.80
2.50	12.02	2.50	5.52
5.00	14.42	5.00	8.35
7.50	16.15	7.50	10.18
10	17.46	10	11.44
15	19.30	15	13.06
20	20.50	20	14.00
25	21.16	25	14.42
30	21.28	30	14.43
35	20.99	35	14.11
40	20.35	40	13.57
45	19.47	45	12.91
50	18.31	50	12.17
55	16.97	55	11.29
60	15.50	60	10.36
65	13.93	65	9.41
70	12.31	70	8.43
75	10.61	75	7.38
80	8.71	80	6.20
85	6.65	85	4.85
90	4.51	90	3.30
95	2.31	95	1.61
100	.20	100	-.20
L.E. radius: 0.293			

NATIONAL ADVISORY
COMMITTEE FOR AERONAUTICS

[redacted]

TABLE XI

APPROXIMATE CRITICAL MACH NUMBERS BASED ON MEAN VELOCITIES

NACA blower-blade section	Solidity	α	q/q_o	M_{cr}
E5-110	0.88	2° 55'	1.5	0.70
65-110	1.00			
65-110	1.50			
65-210	.88	4° 18'	1.5	.70
65-210	1.00			
E5-210	1.50			
E5-410	.88	7° 03'	1.6	.67
65-410	1.00	7° 03'		
65-410	1.50	8° 03'		
65-810	.88	11° 39'	1.7	.64
65-810	1.00	11° 39'		
65-810	1.50	13° 39'		
65-(12)10	.88	16° 08'	1.8	.62
65-(12)10	1.00	16° 08'		
65-(12)10	1.50	18° 08'		
64-(A)06	.976	27°	2.3	.54
64-(A)06	1.465	33°	2.2	.55
64-(B)06	.955	29°	2.3	.54
64-(B)06	1.435	38°	2.5	.51
64-(C)06	.932	41°	3.0	.46
64-(C)06	1.400	44°	3.1	.45
64-(D)06	1.337	61°	8.3	Very low

NATIONAL ADVISORY
COMMITTEE FOR AERONAUTICS

[redacted]

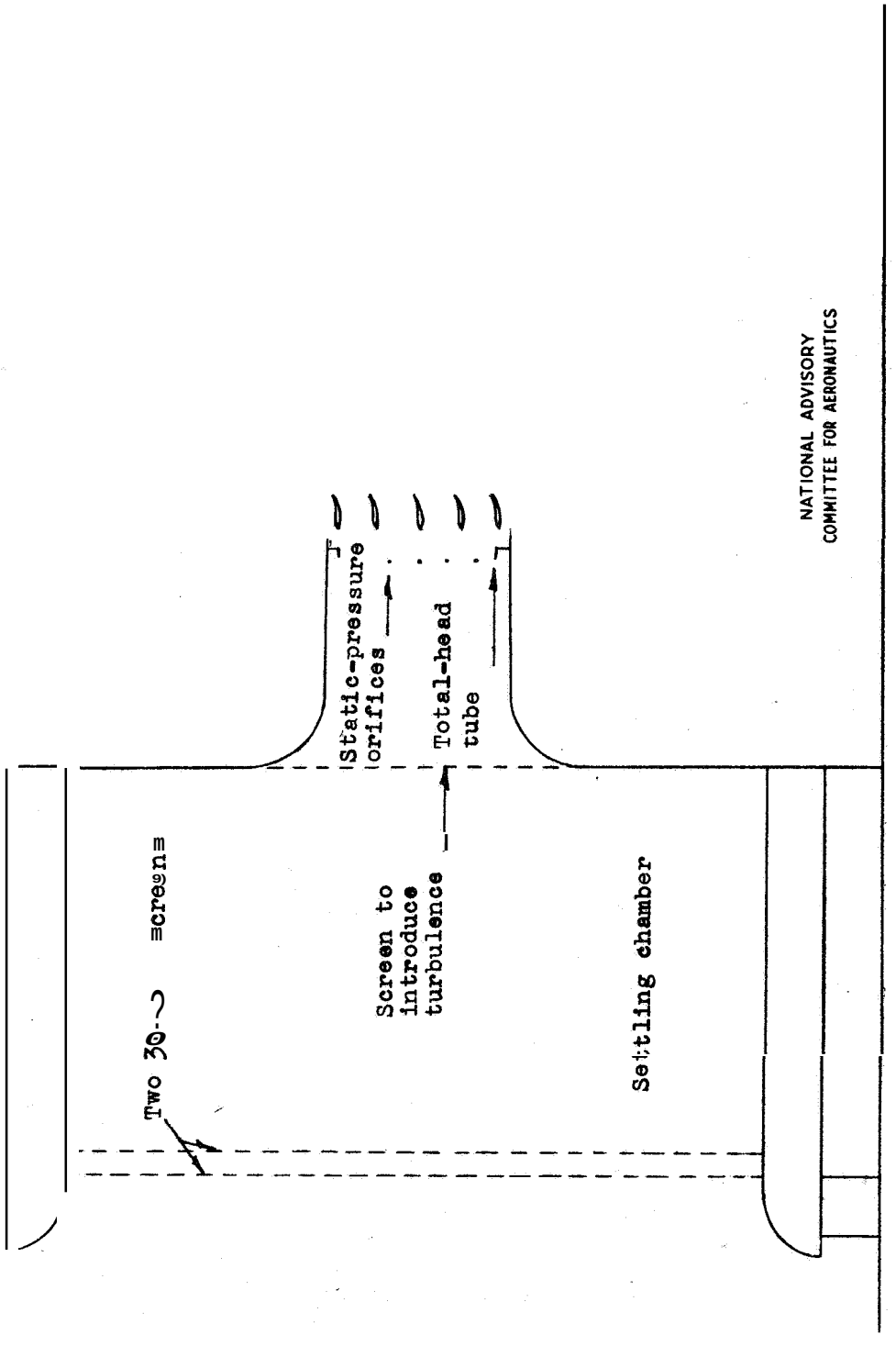

Figure 1.- Two-dimensional low-speed cascade tunnel.

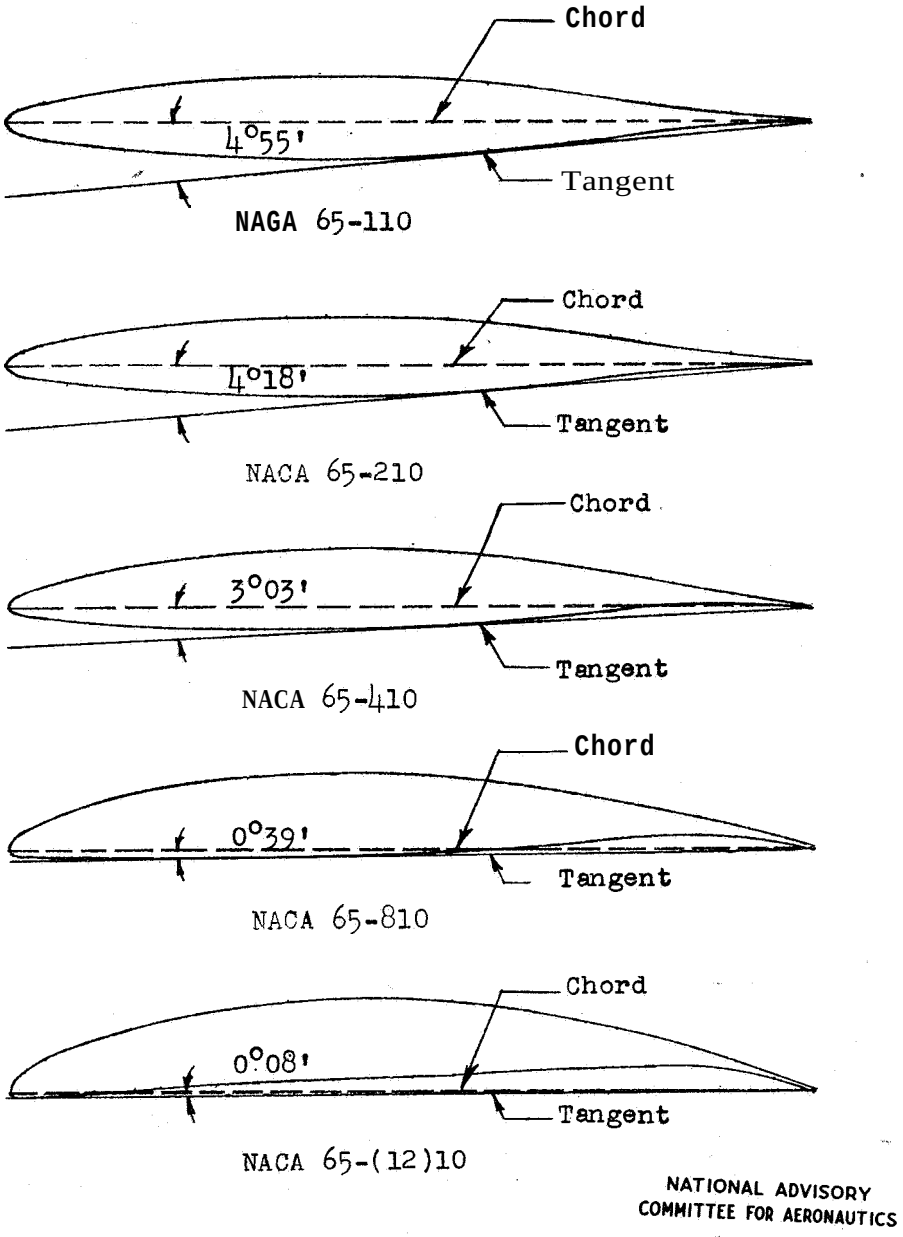

Figure 2.- NACA 65-aeries blower-blade sections.

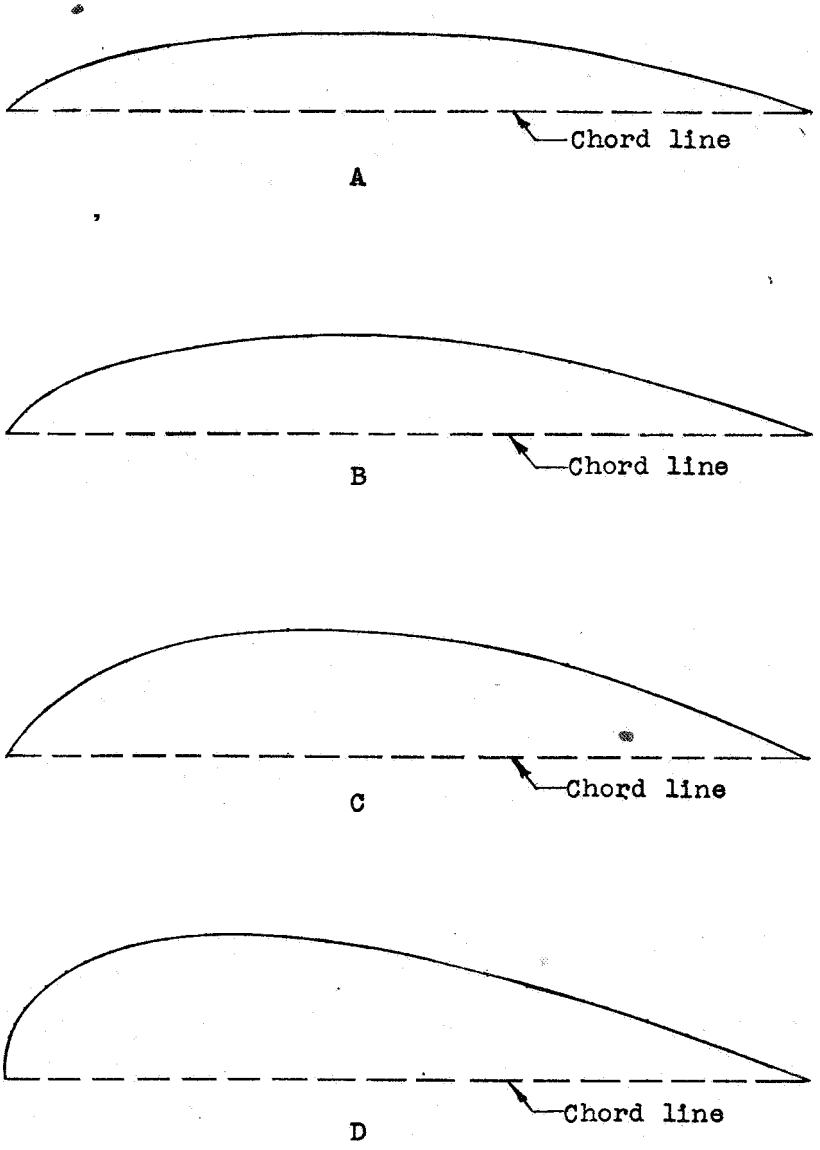

NATIONAL ADVISORY
COMMITTEE FOR AERONAUTICS

Figure 3.- Mean lines obtained from tests of flexible plates in cascade.

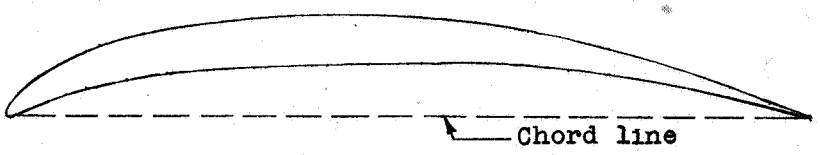

NACA 64-(A)06

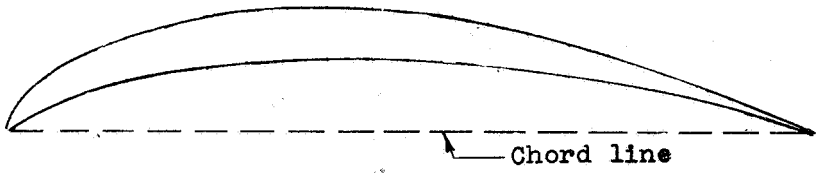

NACA 64-(B)06

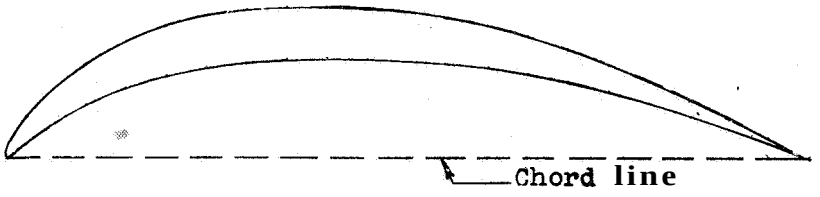

NACA 64-(C)06

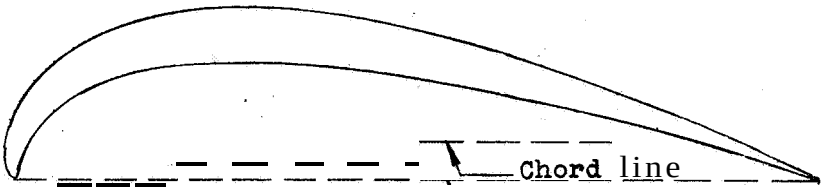

NACA 64-(D)06

NATIONAL ADVISORY
COMMITTEE FOR AERONAUTICS

Figure 4.- Experimentally designed blower-blade sections;

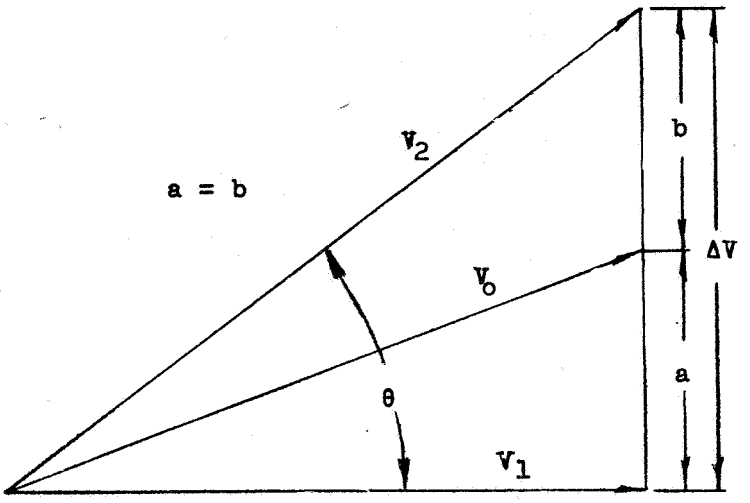

(a) Vector diagram defining mean velocity.

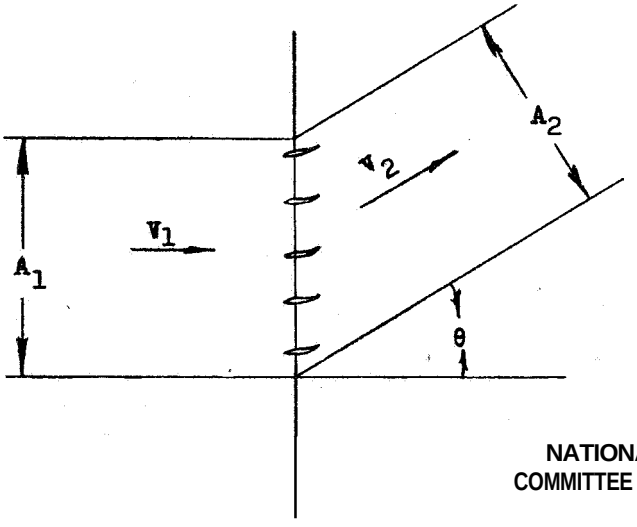

(b) Flow through a cascade of airfoils at 0° stagger.

Figure 5.- Diagrams of flow through a cascade.

o Convex surface
+ Concave surface

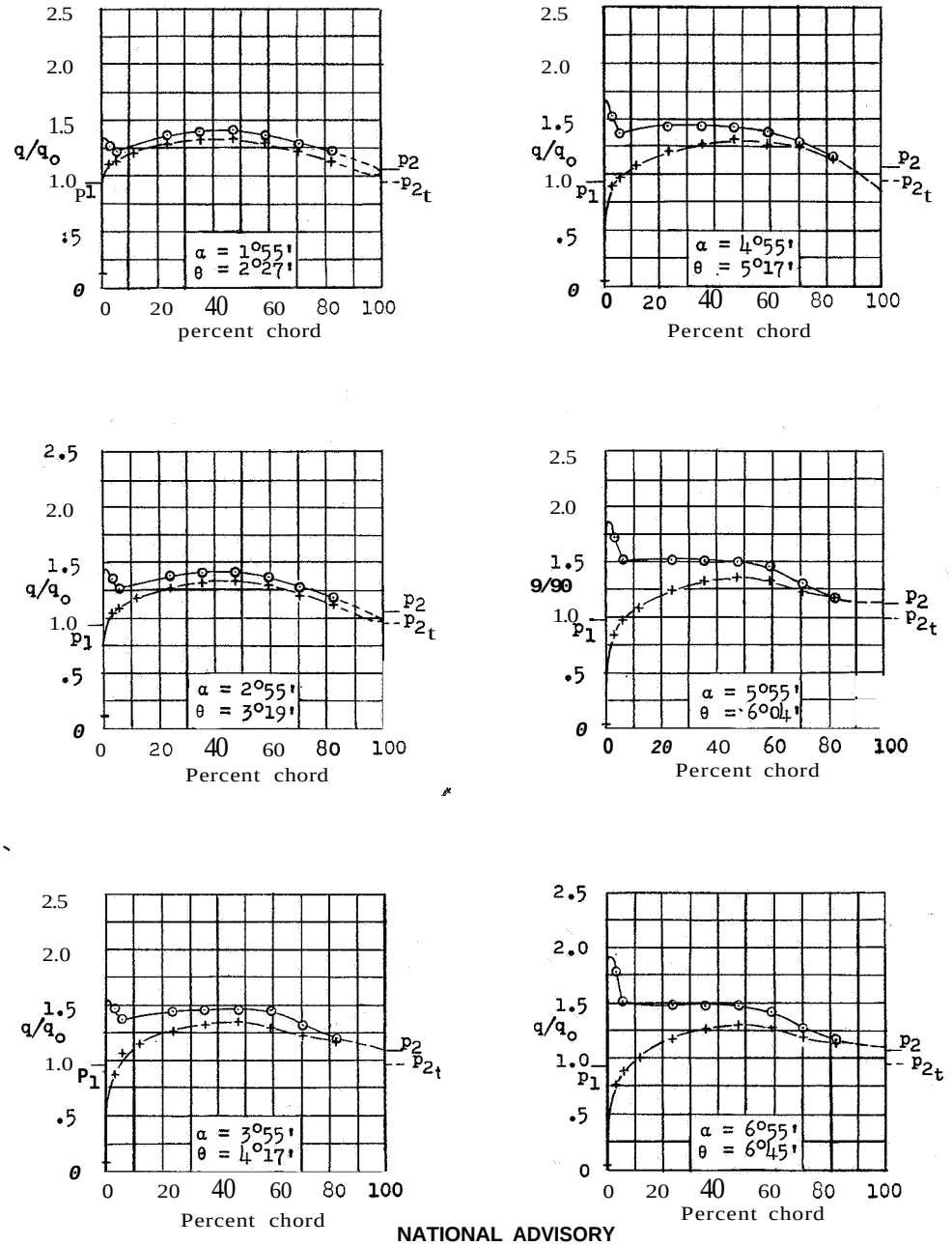

NATIONAL ADVISORY
COMMITTEE FOR AERONAUTICS

Figure 6.- Section pressure distributions for NACA 65-110 blower blade; stagger, 0°; solidity, 0.88; no ad.

a

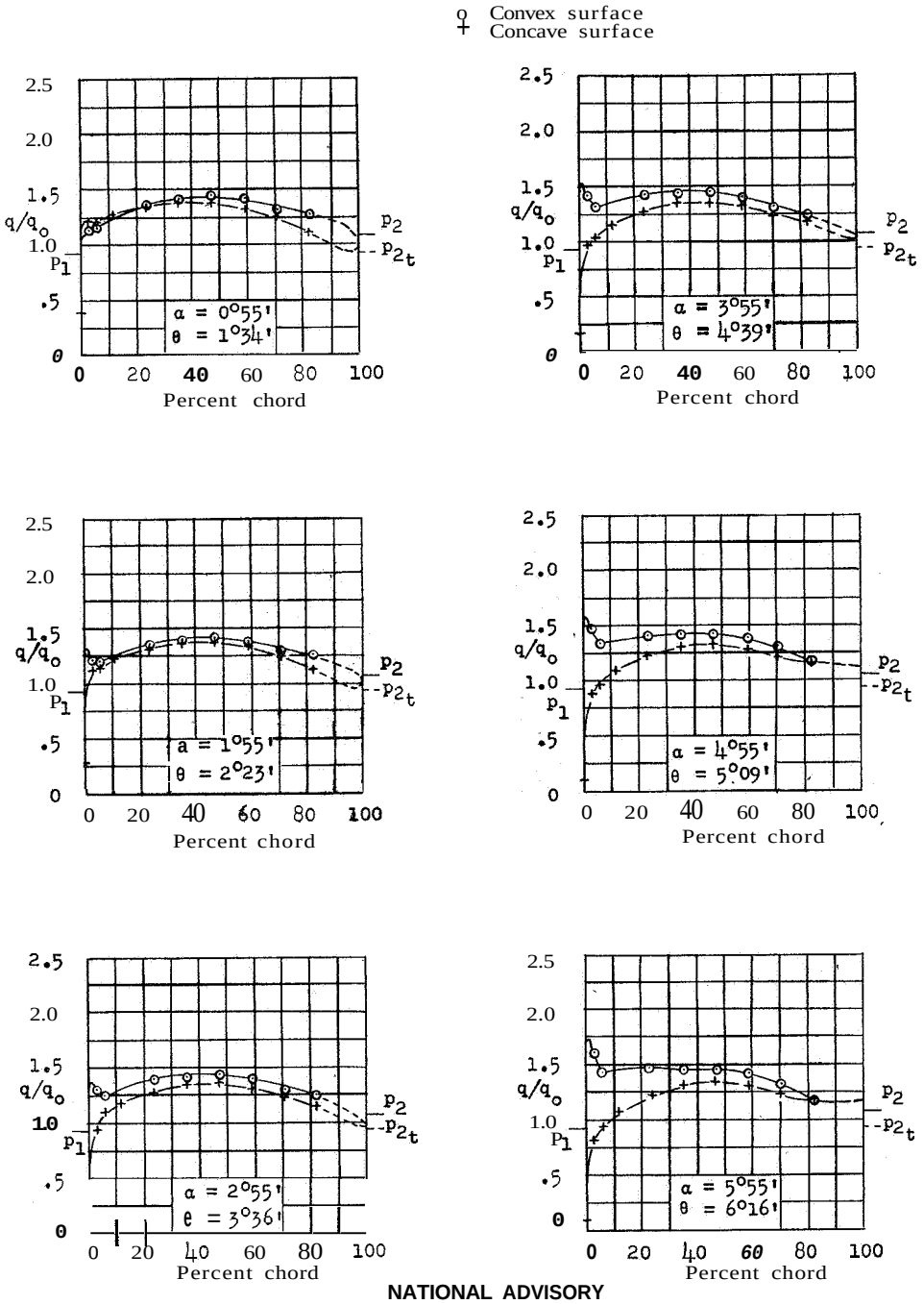

NATIONAL ADVISORY
COMMITTEE FOR AERONAUTICS.

Figure 7.- Section pressure distributions for NACA 65-110 blower blade; stagger, 0°; solidity, 1.00; no α_d.

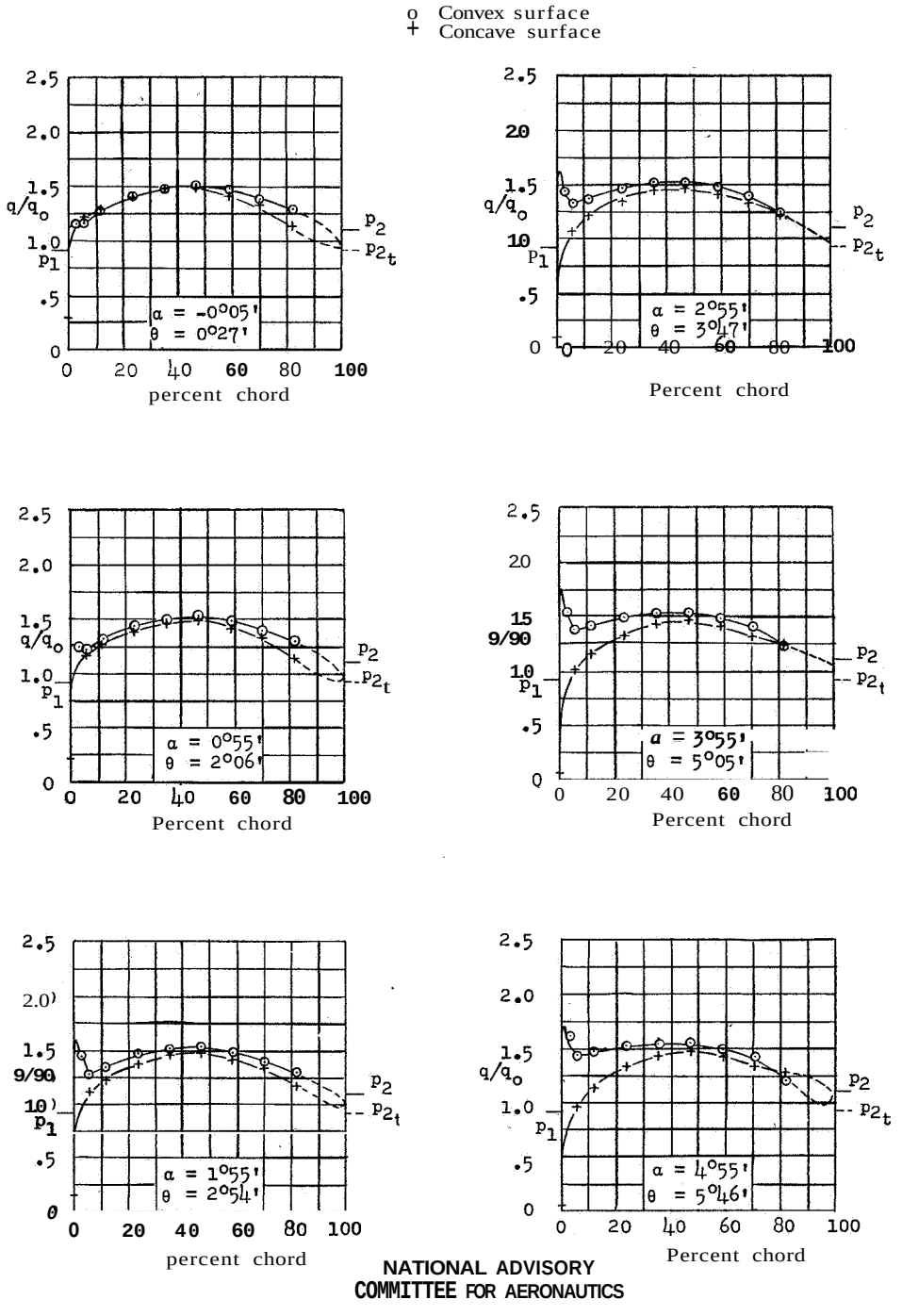

Figure 8.- Section pressure distributions for NACA 65-110 blower blade; stagger, 0°; solidity, 1.50; no α_d.

o Convex surface
+ concave surface

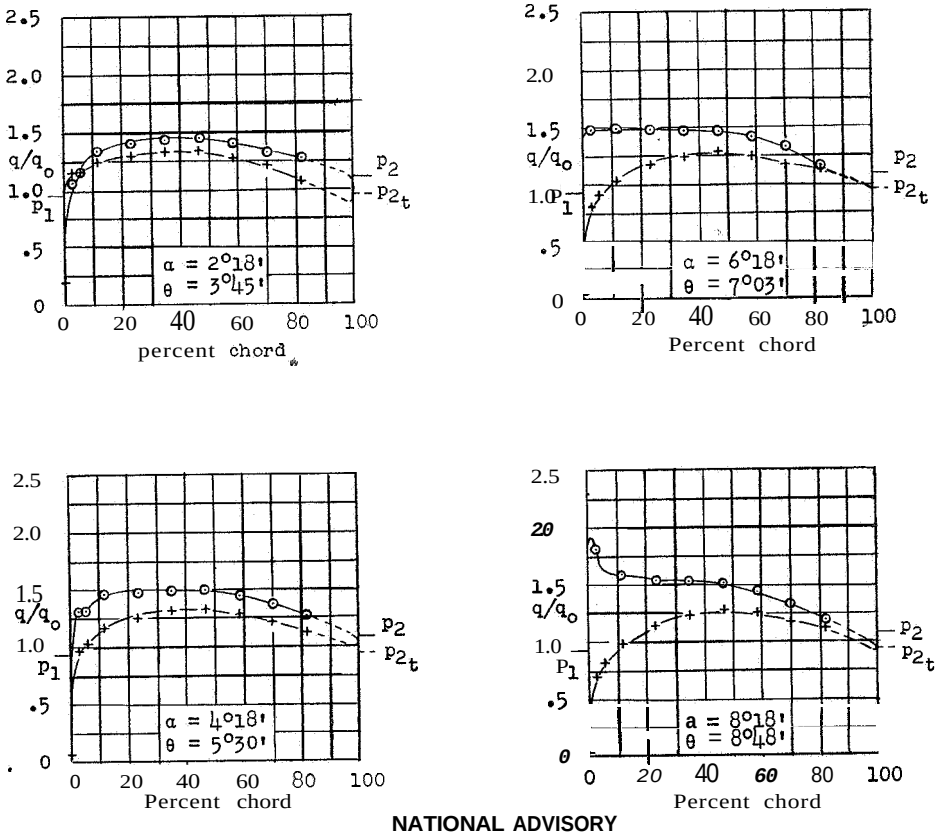

NATIONAL ADVISORY
COMMITTEE FOR AERONAUTICS

Figure 9.- Section pressure distributions for NACA 65-210 blower blade; stagger, 0°; solidity, 0.88; $\alpha_d = 4°18'$.

o Cdnvex surface
+ Concave surface

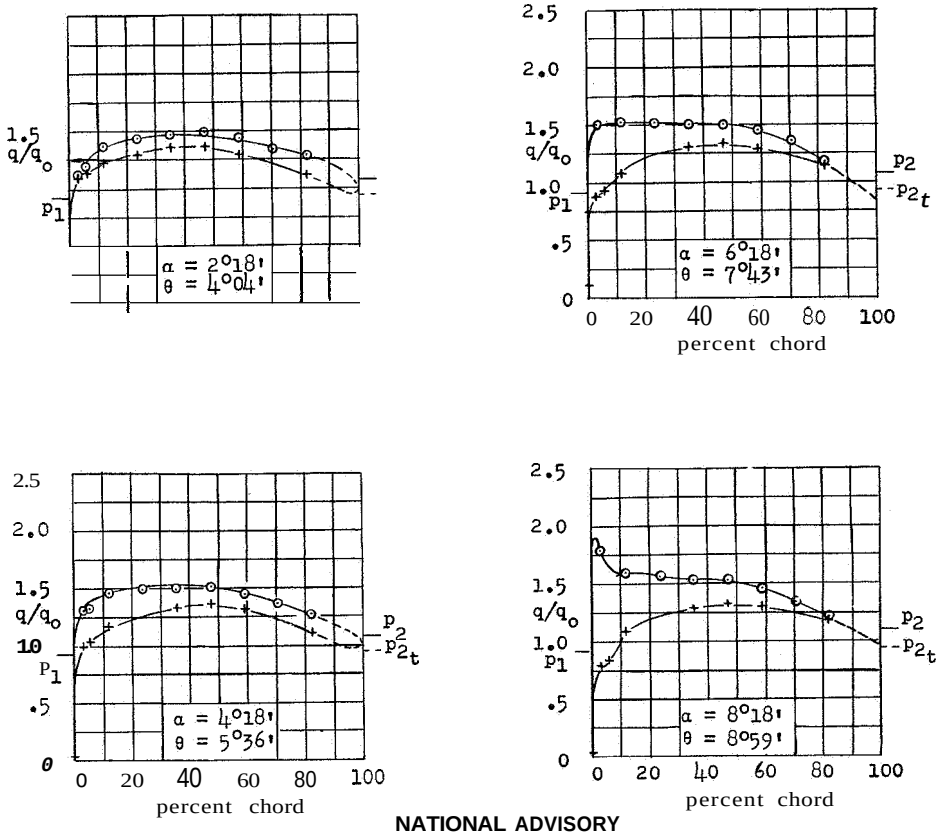

NATIONAL ADVISORY
COHHITTEE FOR AERONAUTICS

Figure 10.- Section pressure distributions for NACA 65-210 blower blade; stagger, 0°; solidity, 1.00; $\alpha_d = 4°18'$.

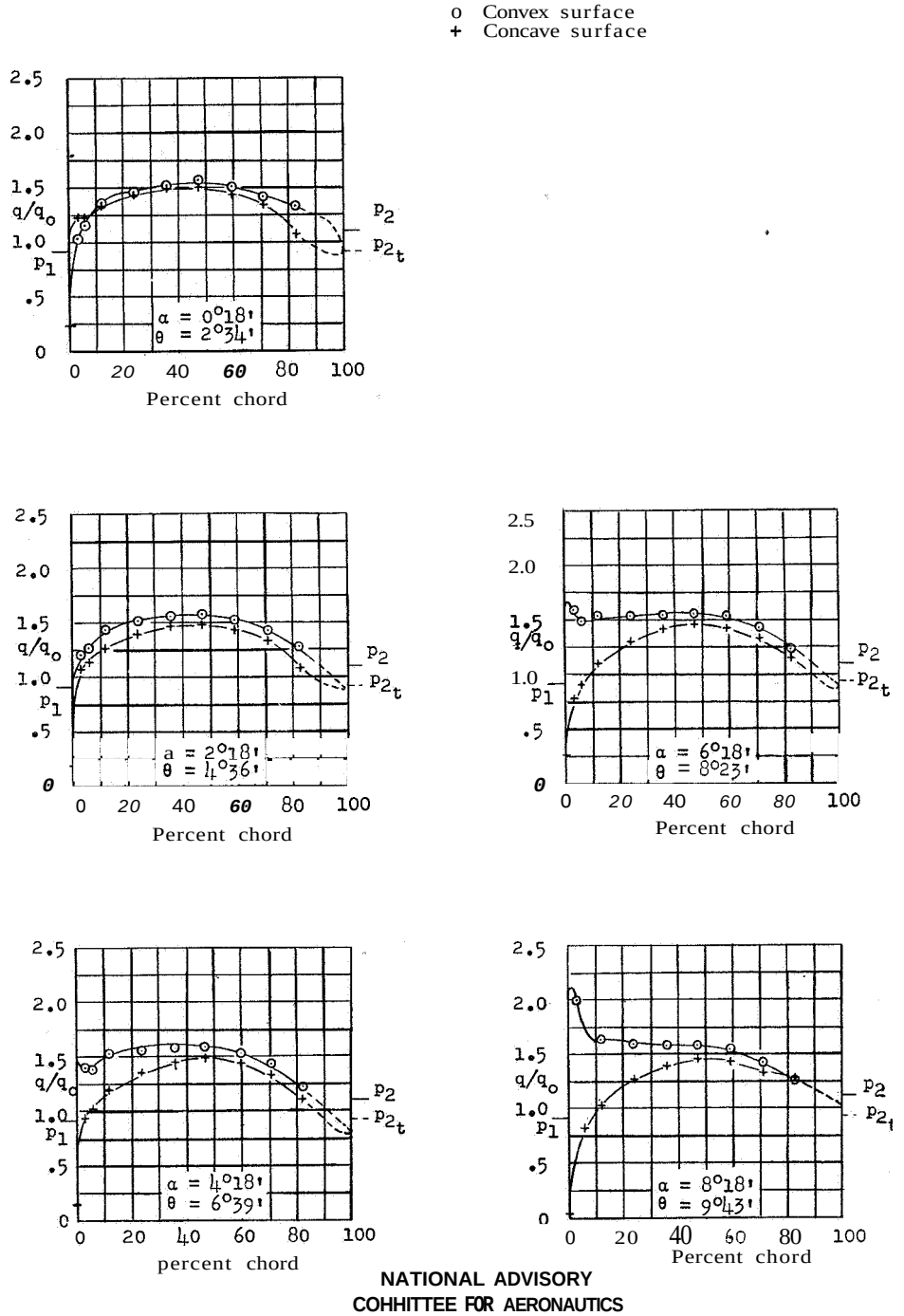

NATIONAL ADVISORY
COHHITTEE FOR AERONAUTICS

Figure 11.- Section pressure distributions for NACA 65-210 blower blade: stagger, 0°; solidity, 1.50; $\alpha_d = 4°18'$.

o Convex surface
+ Concave surface

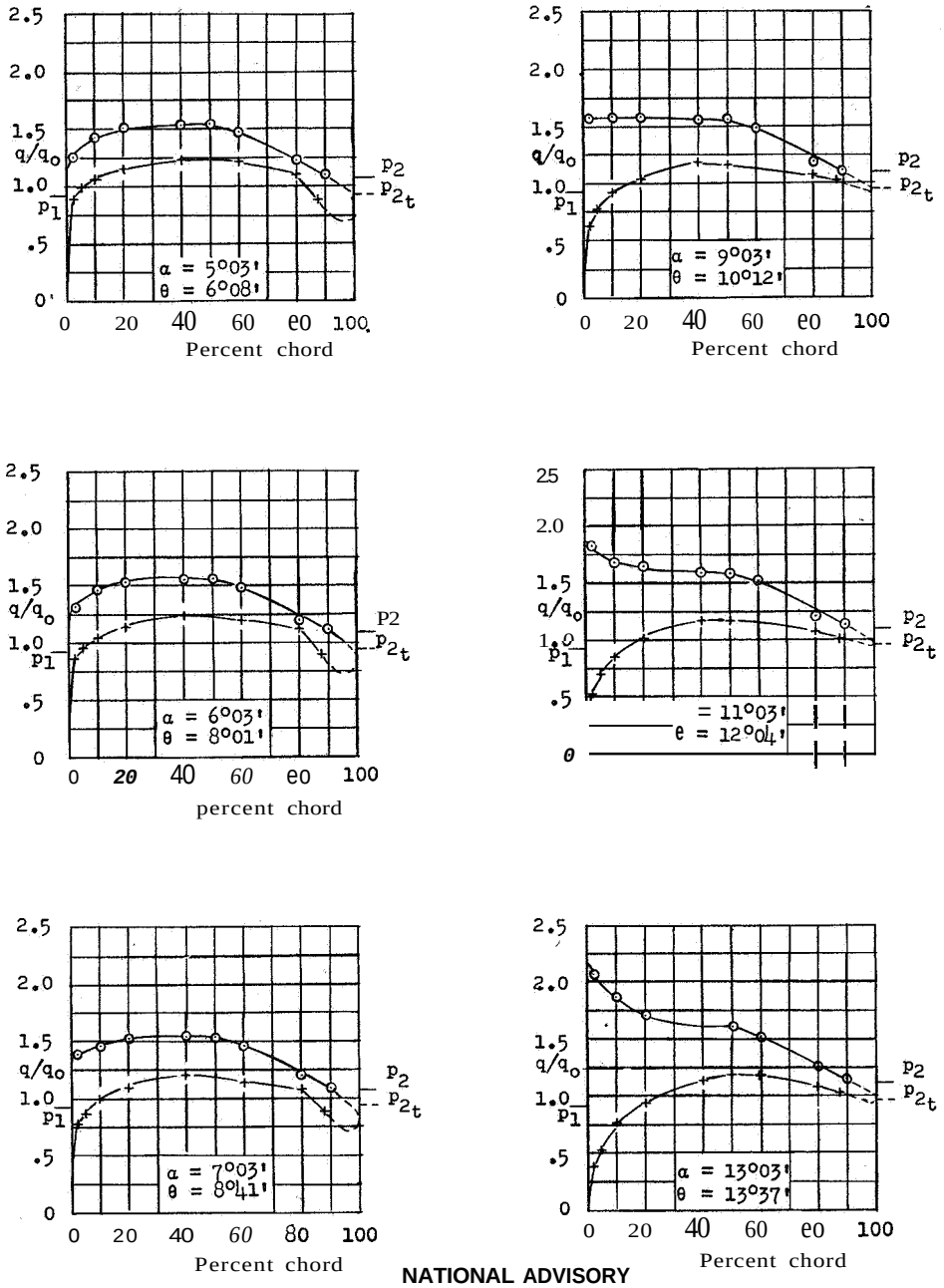

NATIONAL ADVISORY COMMITTEE FOR AERONAUTICS

Figure 12.- Section pressure distributions for NACA 65-410 blower blade; stagger, 0°; solidity, 0.88; $\alpha_d = 7°03'$.

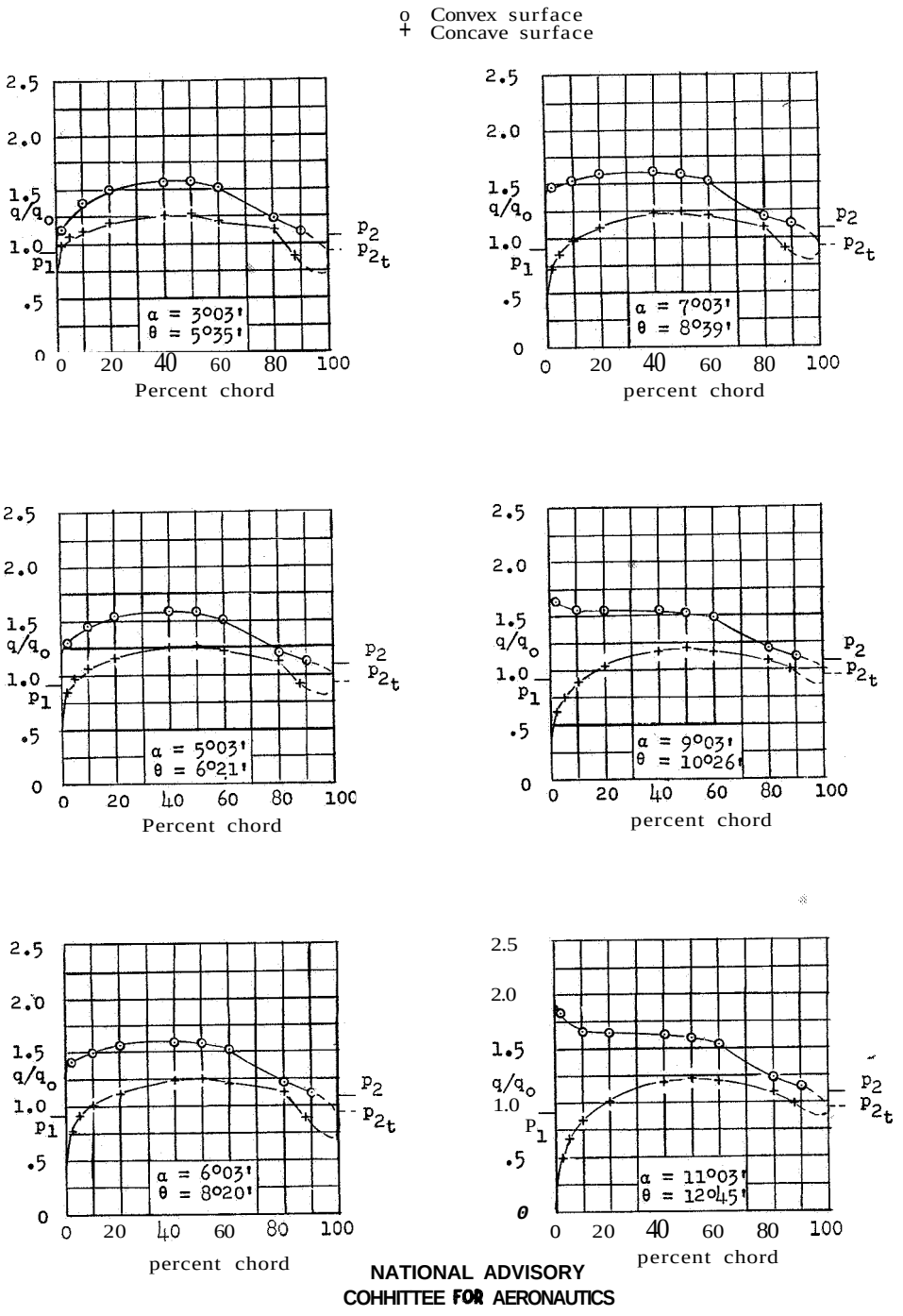

Figure 13.- Section pressure distributions for NACA 65-410 blower blade; stagger, 0°; solidity, 1.00; $\alpha_d = 7°03'$.

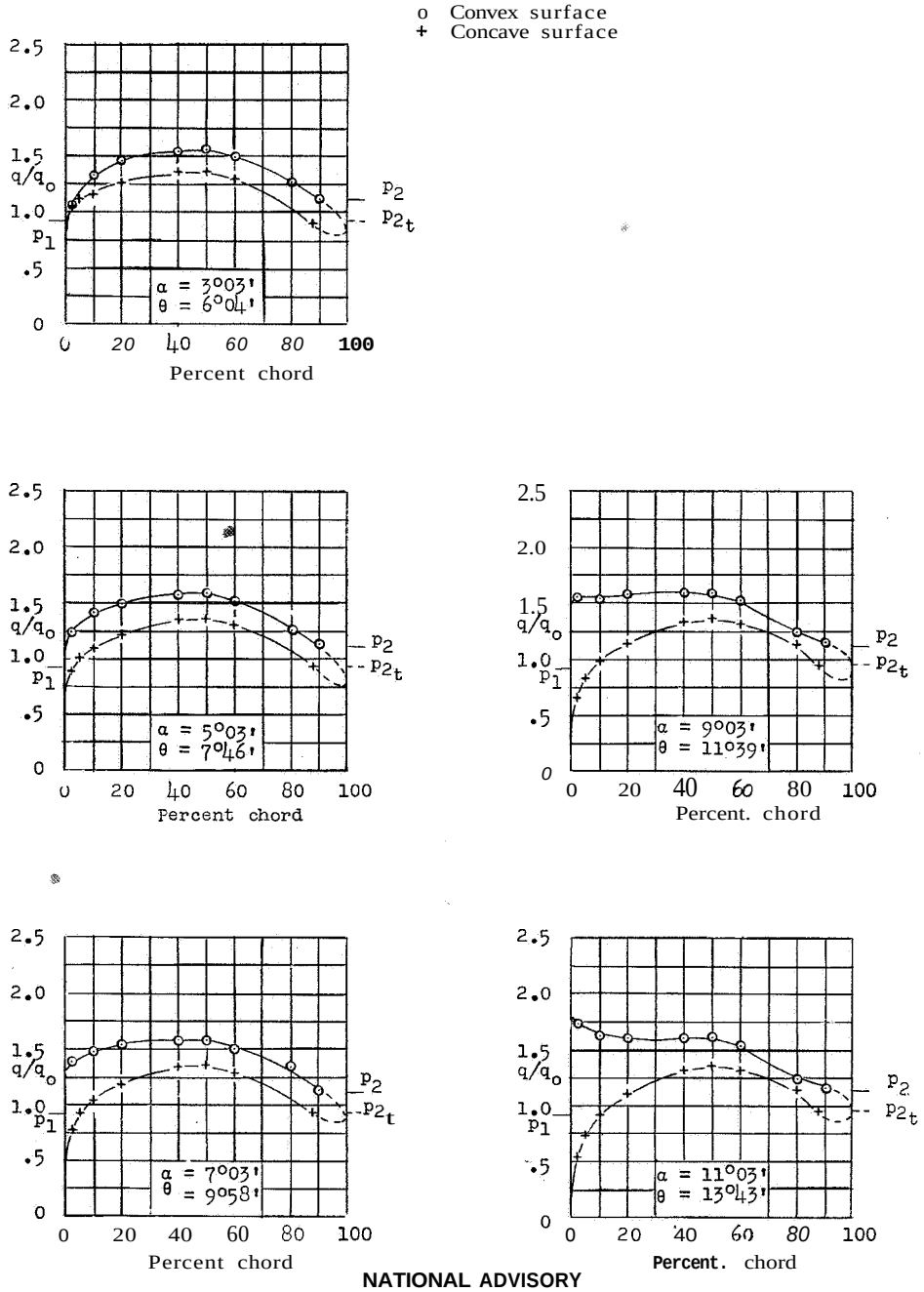

NATIONAL ADVISORY
COHHITTEE FOR AERONAUTICS

Figure 14.- Section pressure distributions for NACA 65-410 blower blade; stagger, 0°; solidity, 1.50; α_d = 8°03'.

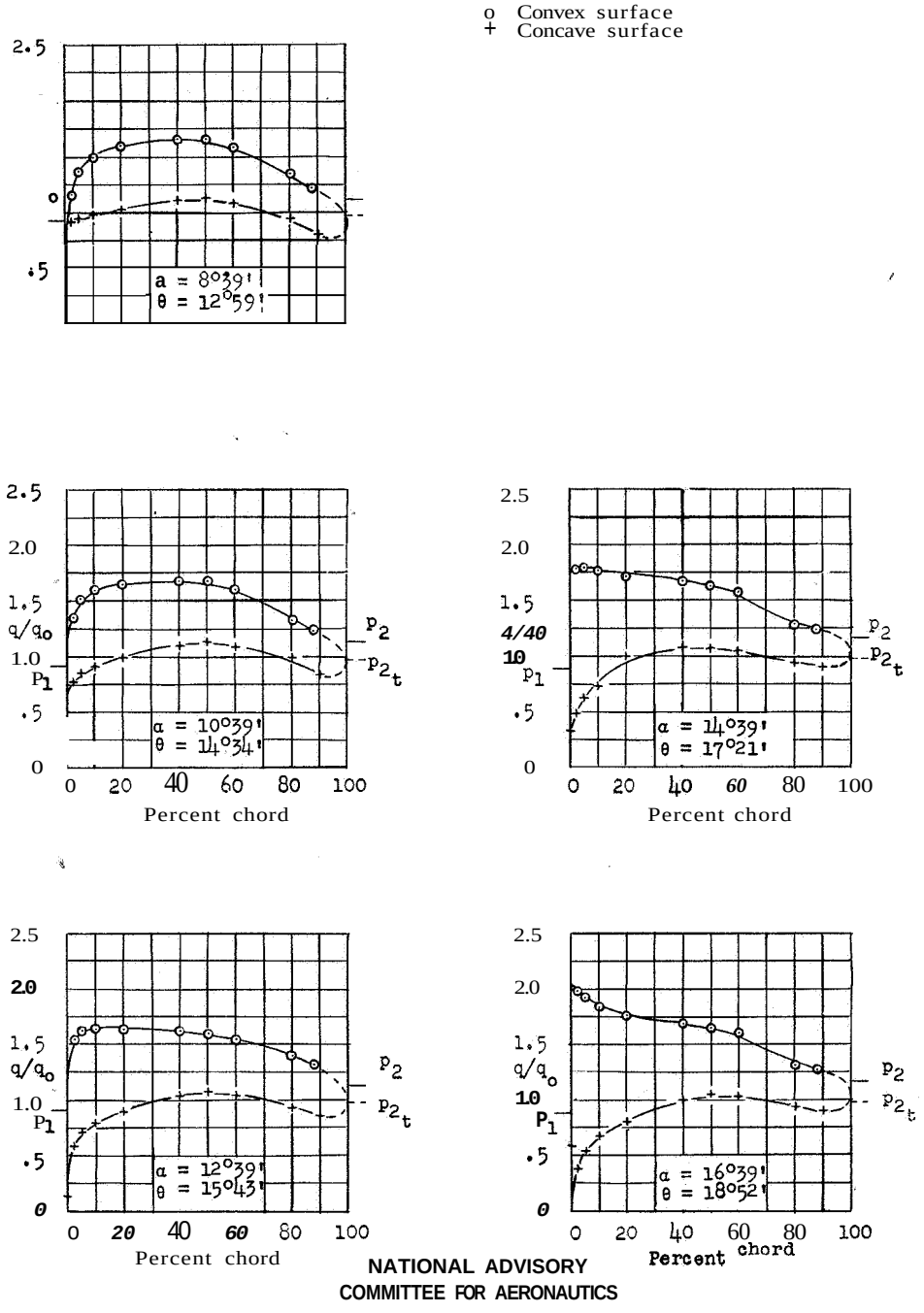

Figure 15.- Section pressure distributions for NACA 65-810 blower blade; stagger, 0°; solidity, 0.88; α_d = 11°39'.

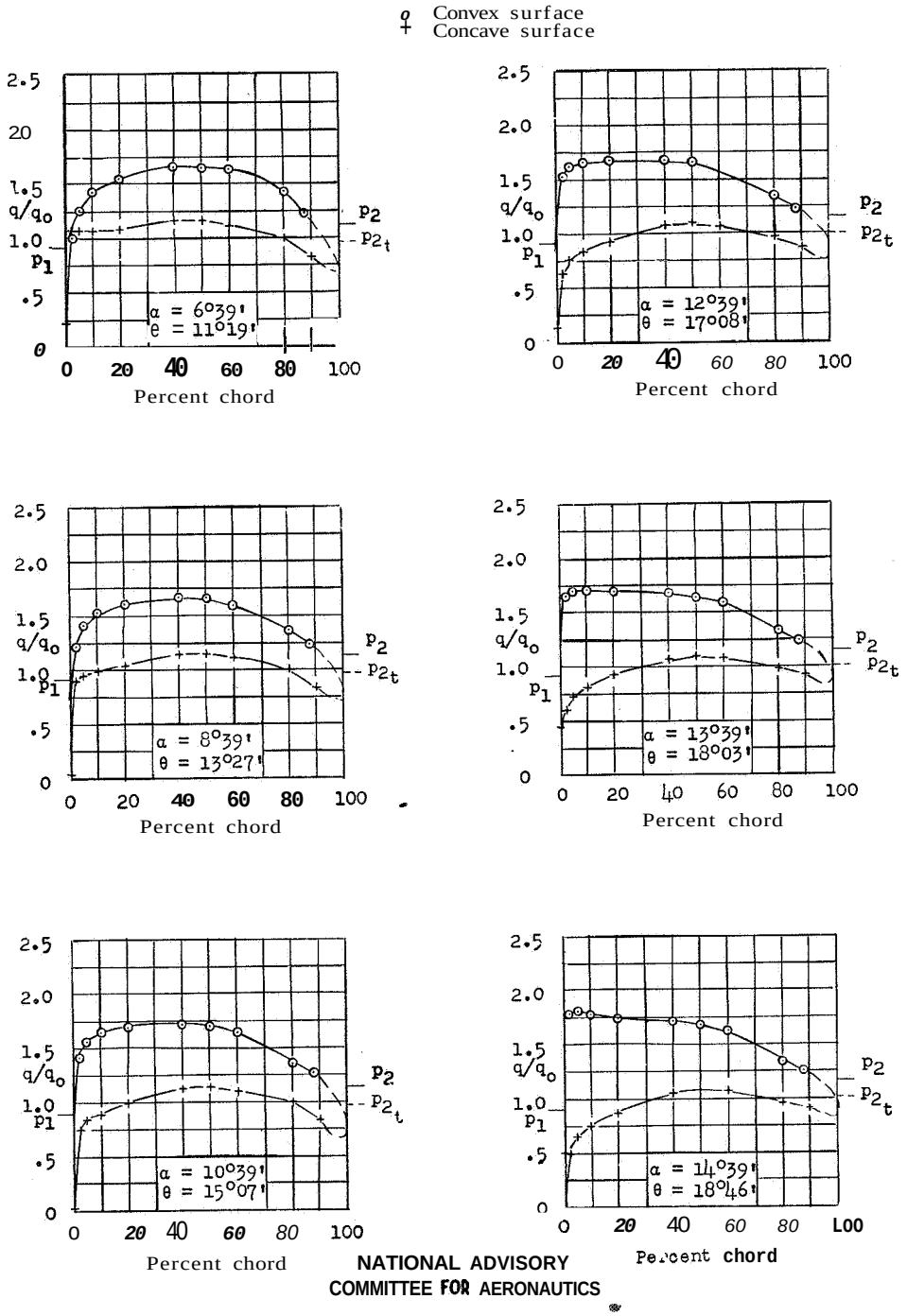

Figure 16.- Section pressure distributions for NACA 65-810 blower blade; stagger, 0°; solidity, 1.00; α_d = 11°39'.

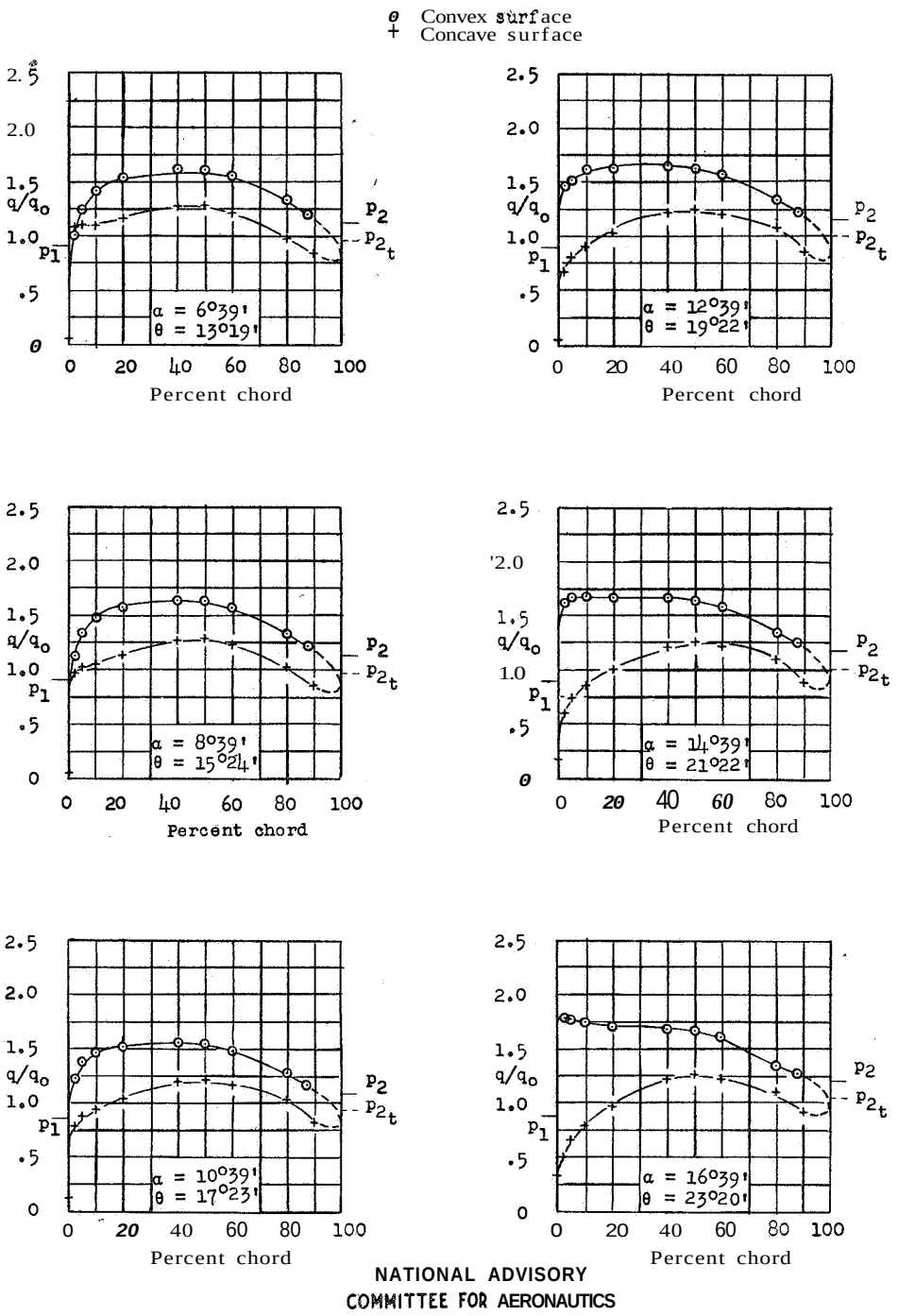

Figure 17.- Section pressure distributions for NACA 65-810 blower blade; stagger, 0°; solidity, 1.50; α_d = 13°39'.

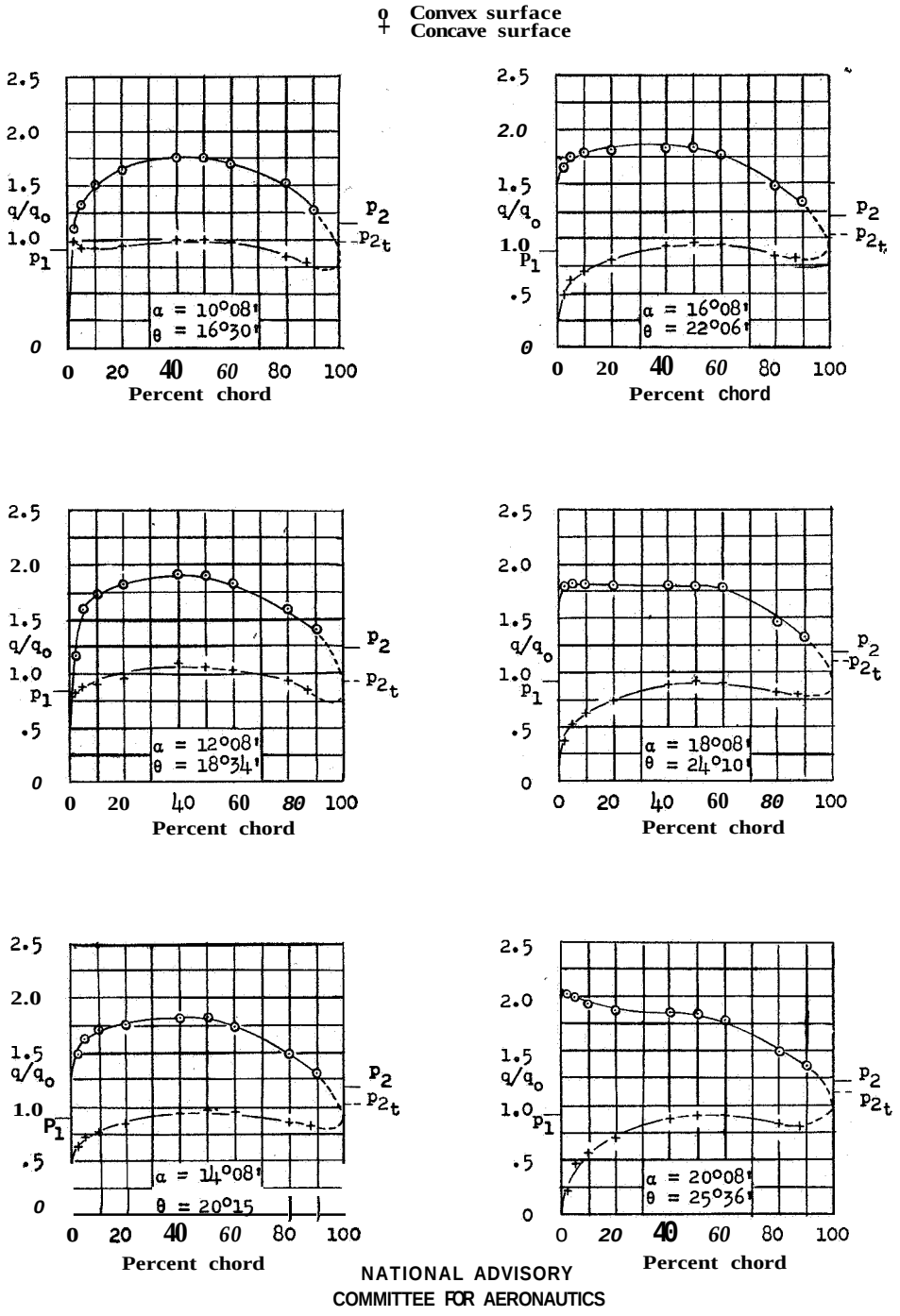

Figure 16.- Section pressure distributions for NACA 65-(12)10 **blower blade; stagger, 0°; solidity,** *0.68;* $\alpha_d = 16°08'$.

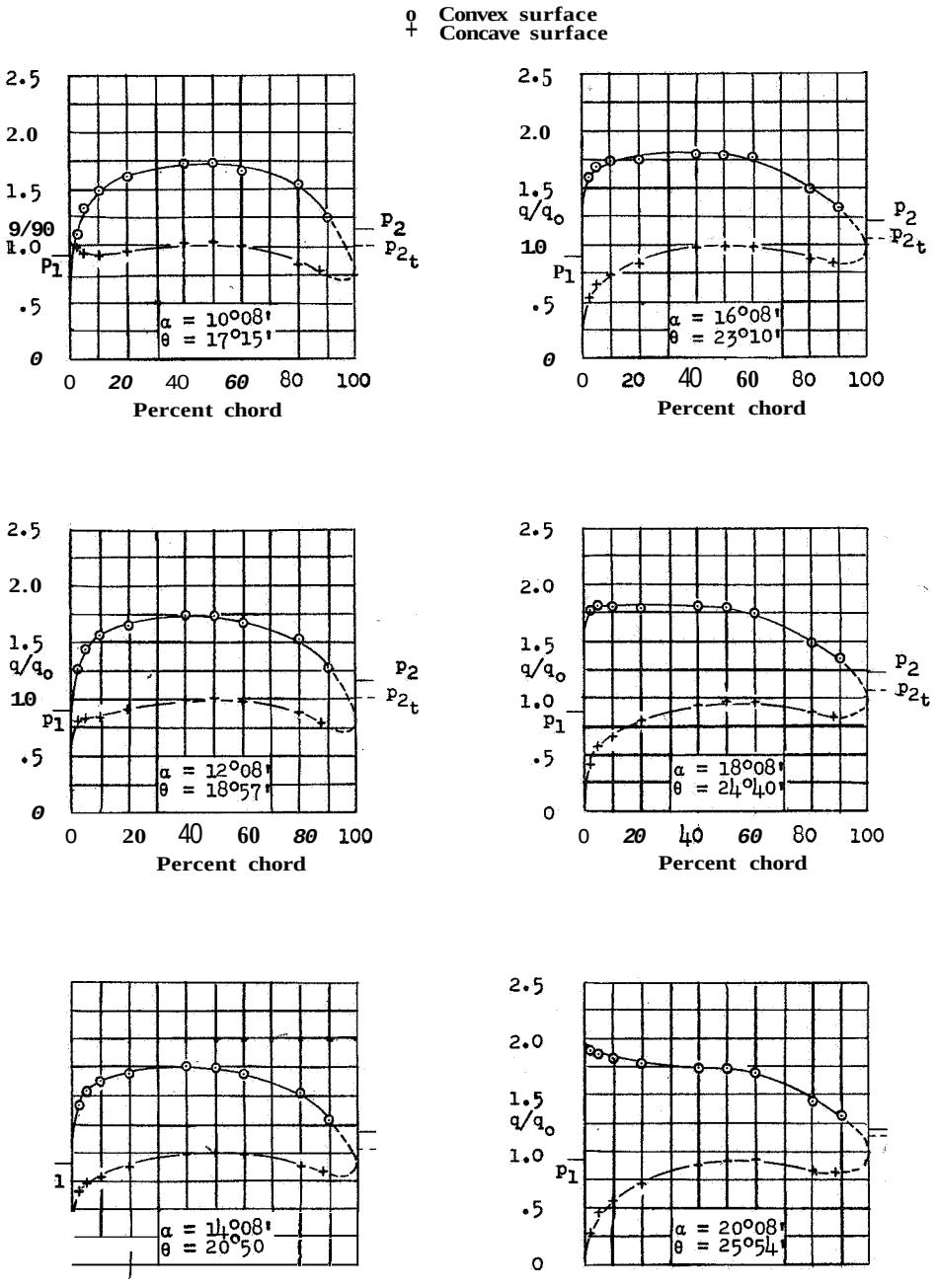

Figure 19.- Section pressure distributions for NACA 65-(12)10 blower blade; stagger, 0°; solidity, 1.00; α_d = 16°08'.

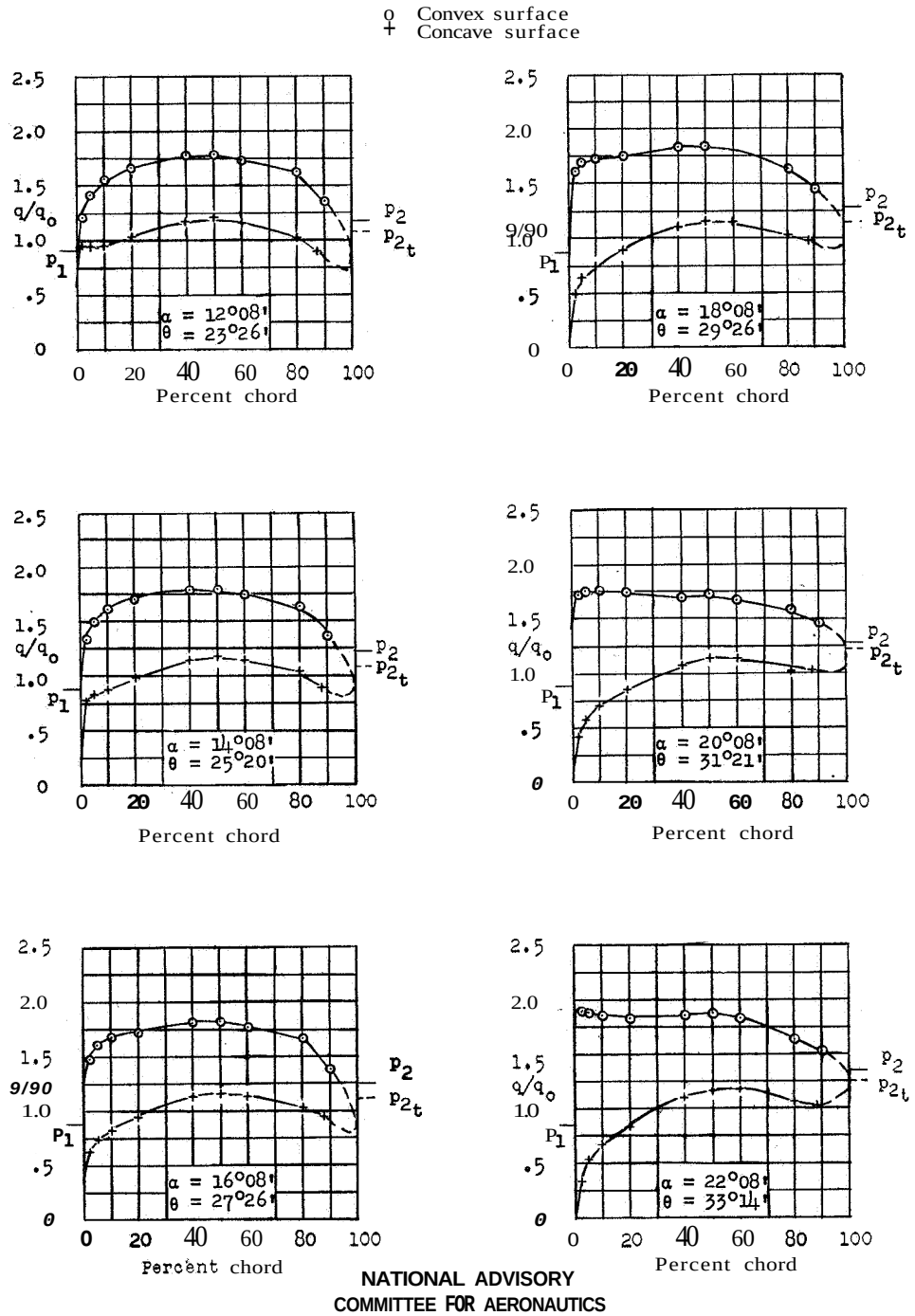

Figure 20.– Section pressure distributions for NACA 65-(12)10 blower blade; stagger, 0°; solidity, 1.50; α_d = 18°08'.

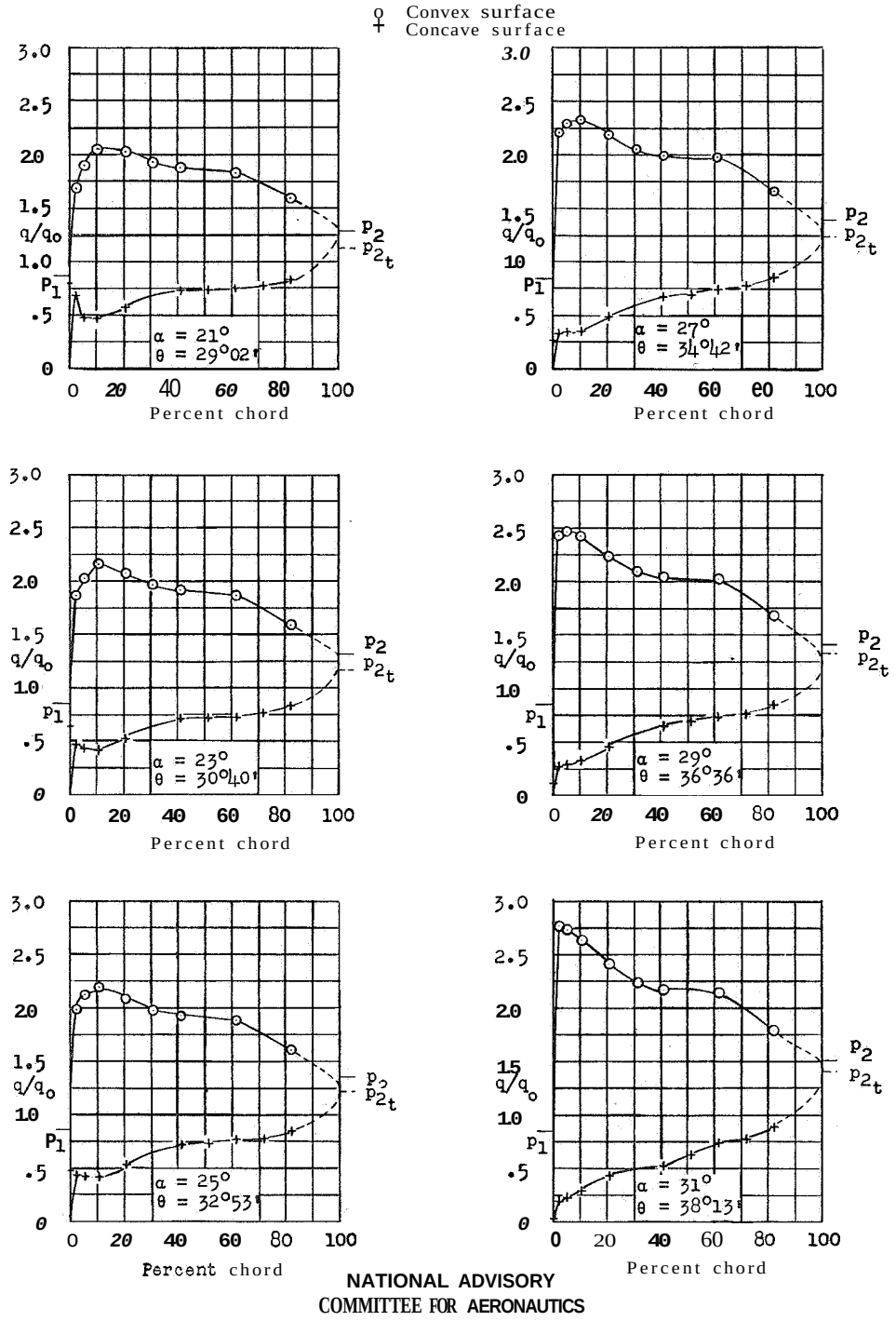

Figure 21.- Section pressure distributions for experimentally designed blower blade NACA 64-(A)06; stagger, 0°; solidity, 0.976; no oecommended design condition.

o Convex surface
+ Concave surface

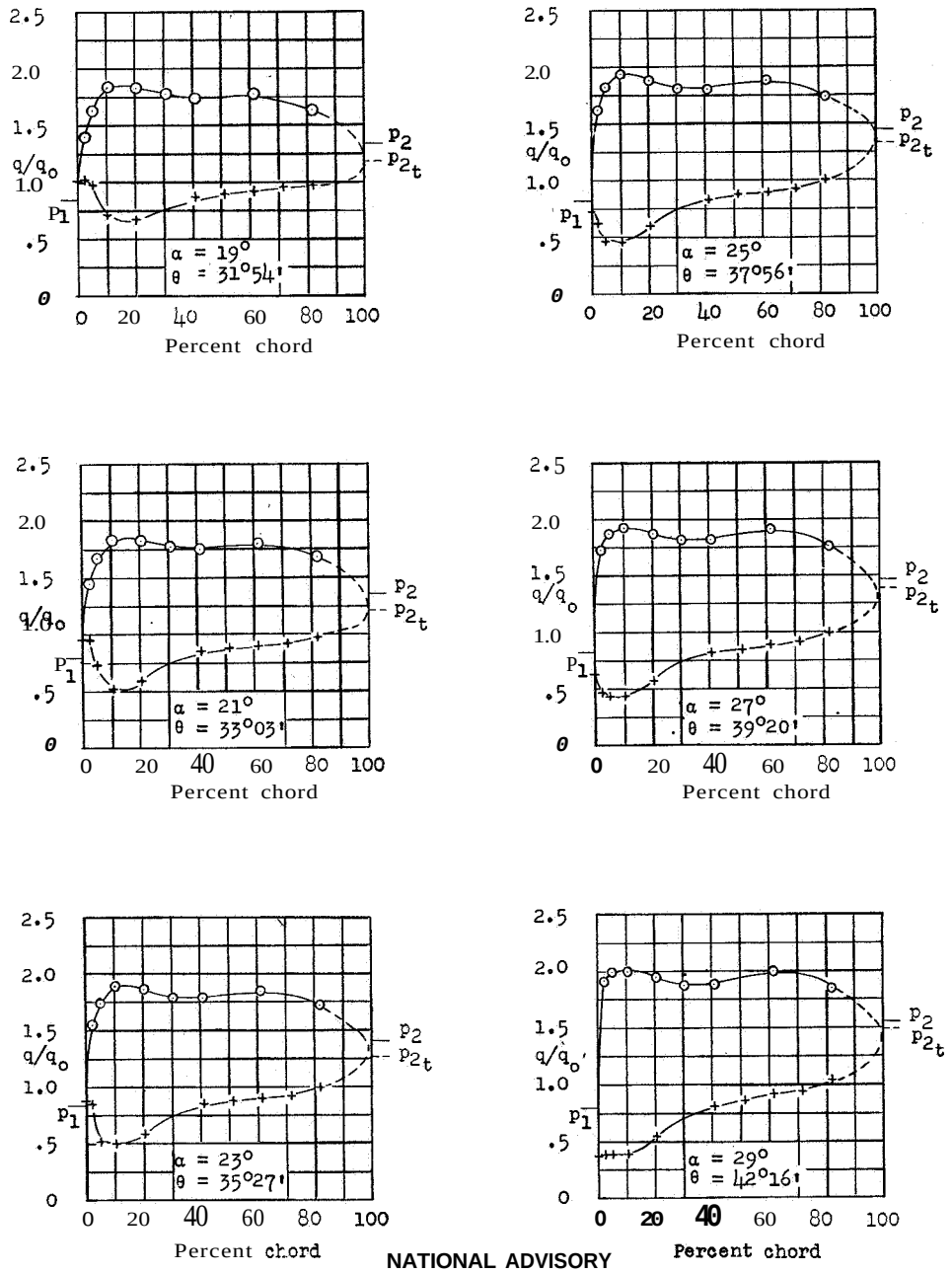

NATIONAL ADVISORY
COMMITTEE FOR AERONAUTICS

Figure 22.- Section pressure distributions for experinentally designed blower blade NACA 64-(A)06; stagger, 0°; solidity, 1.465; range of α_d, 21° to 33°.

o Convex surface
+ Concave surface

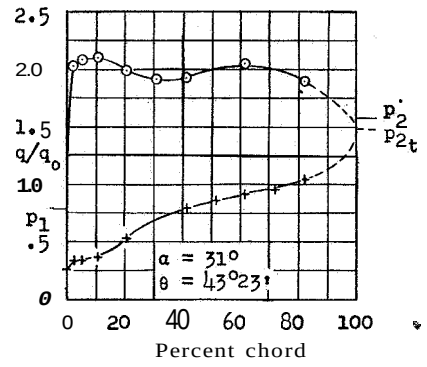

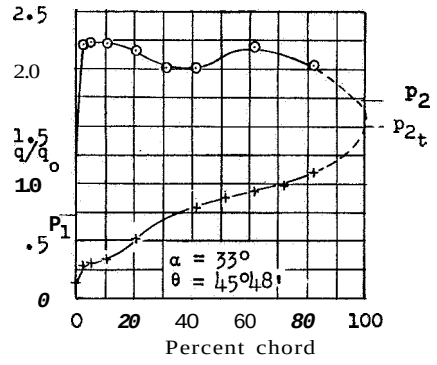

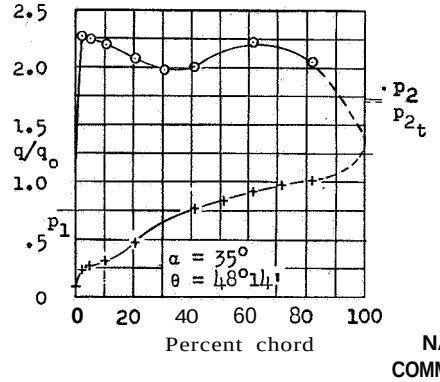

NATIONAL ADVISORY
COMMITTEE FOR AERONAUTICS

Figure 22.- Concluded.

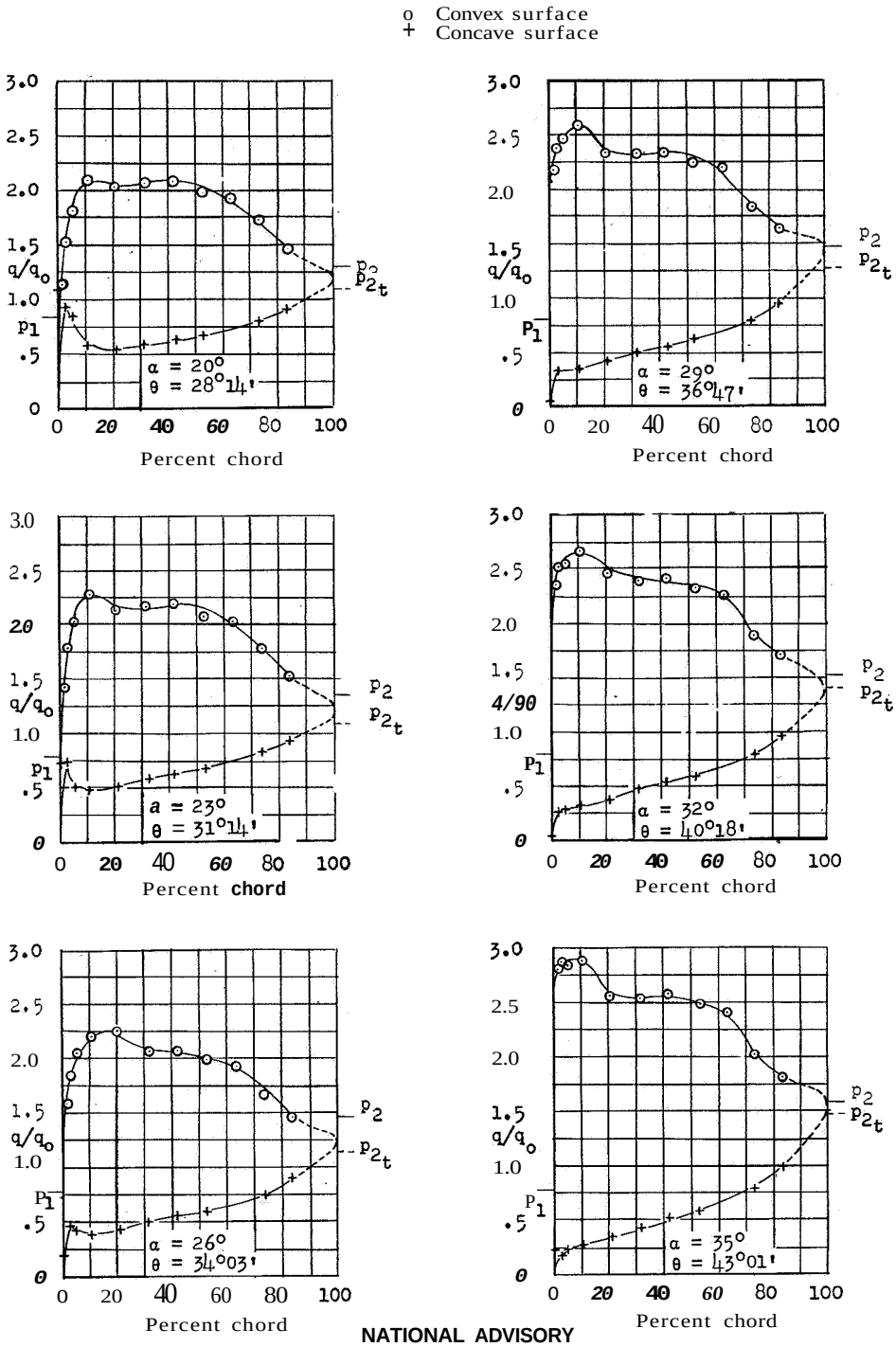

NATIONAL ADVISORY
COMMITTEE FOR AERONAUTICS

Figure 23.- Section pressure distributions for experimentally designed blower blade NACA 64-(B)06; stagger, 0°; solidity, 0.955: no recommended design condition.

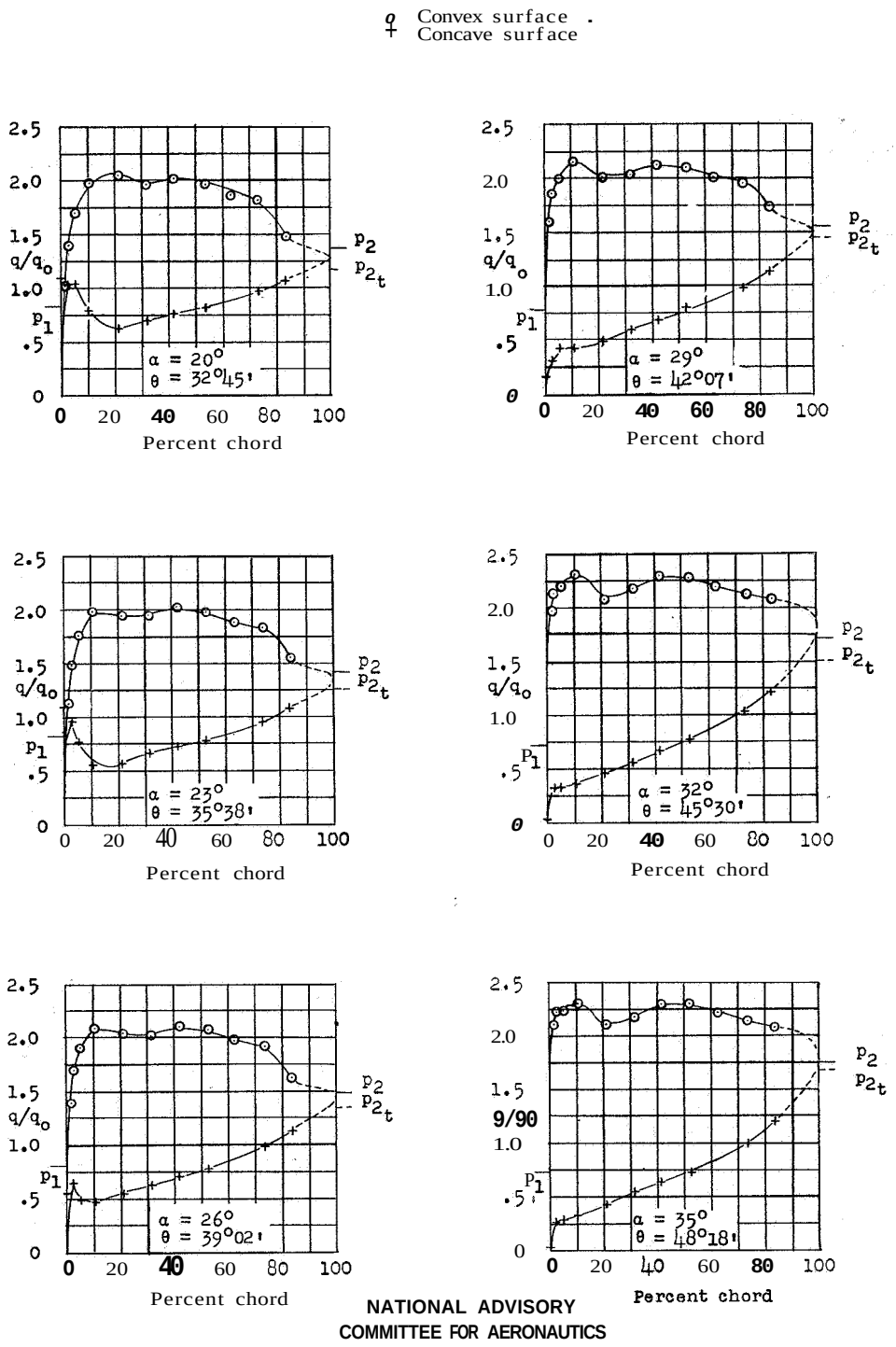

Figure 24.- Section pressure distributions for experimentally designed blower blade NACA 64-(B)06; stagger, 0°; solidity, 1.435; range of ad, 26° to 38°.

o Convex surfaoe
+ Concave surface

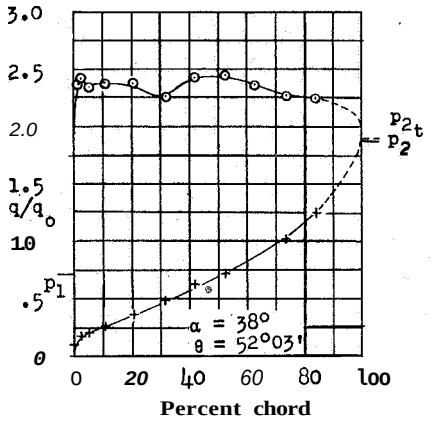

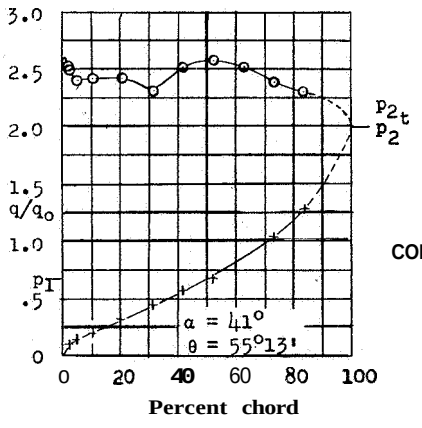

NATIONAL ADVISORY
COMMITTEE FOR AERONAUTICS

Figure 24.- Concluded.

o Convex surface
+ Concave surface

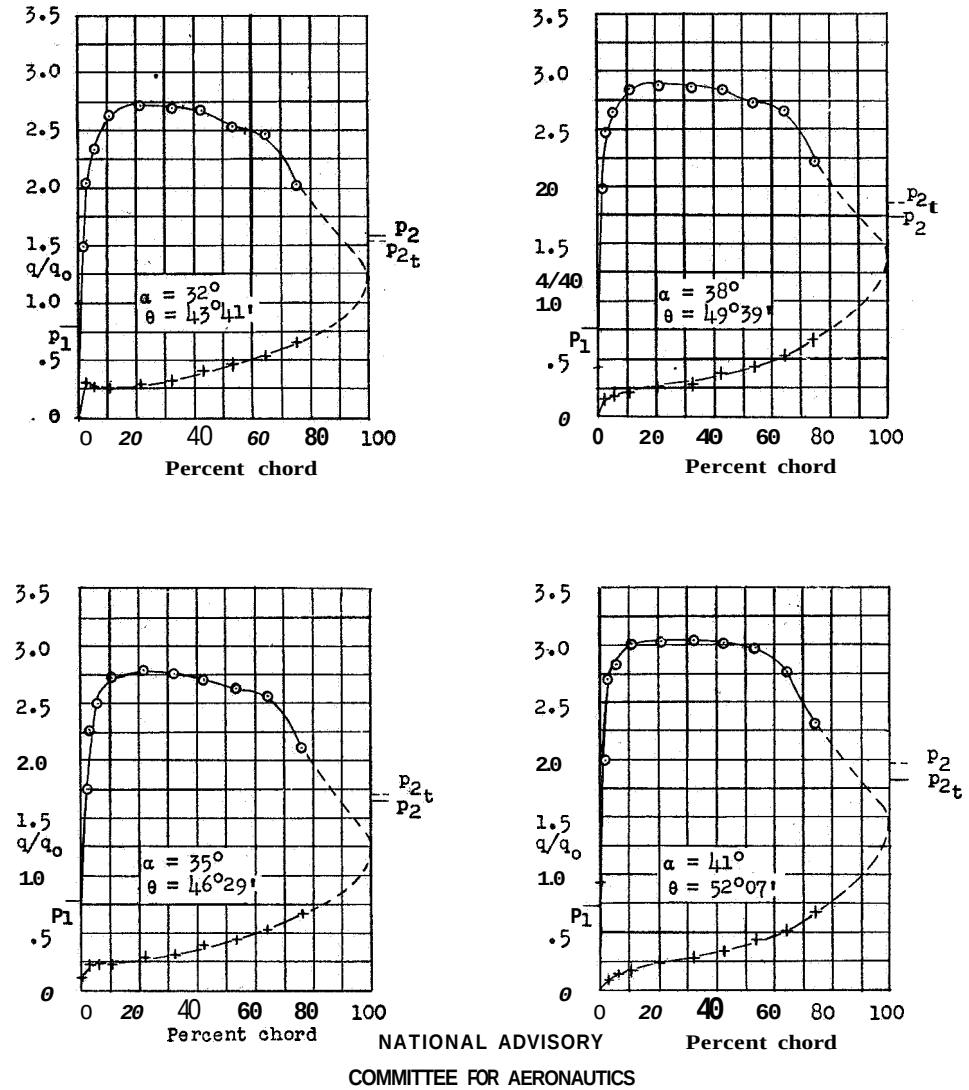

Figure 25. - Section pressure distributions for experimentally designed blower blade NACA 64-(C)06; stagger, 0°; solidity, 0.932; no recommended design condition.

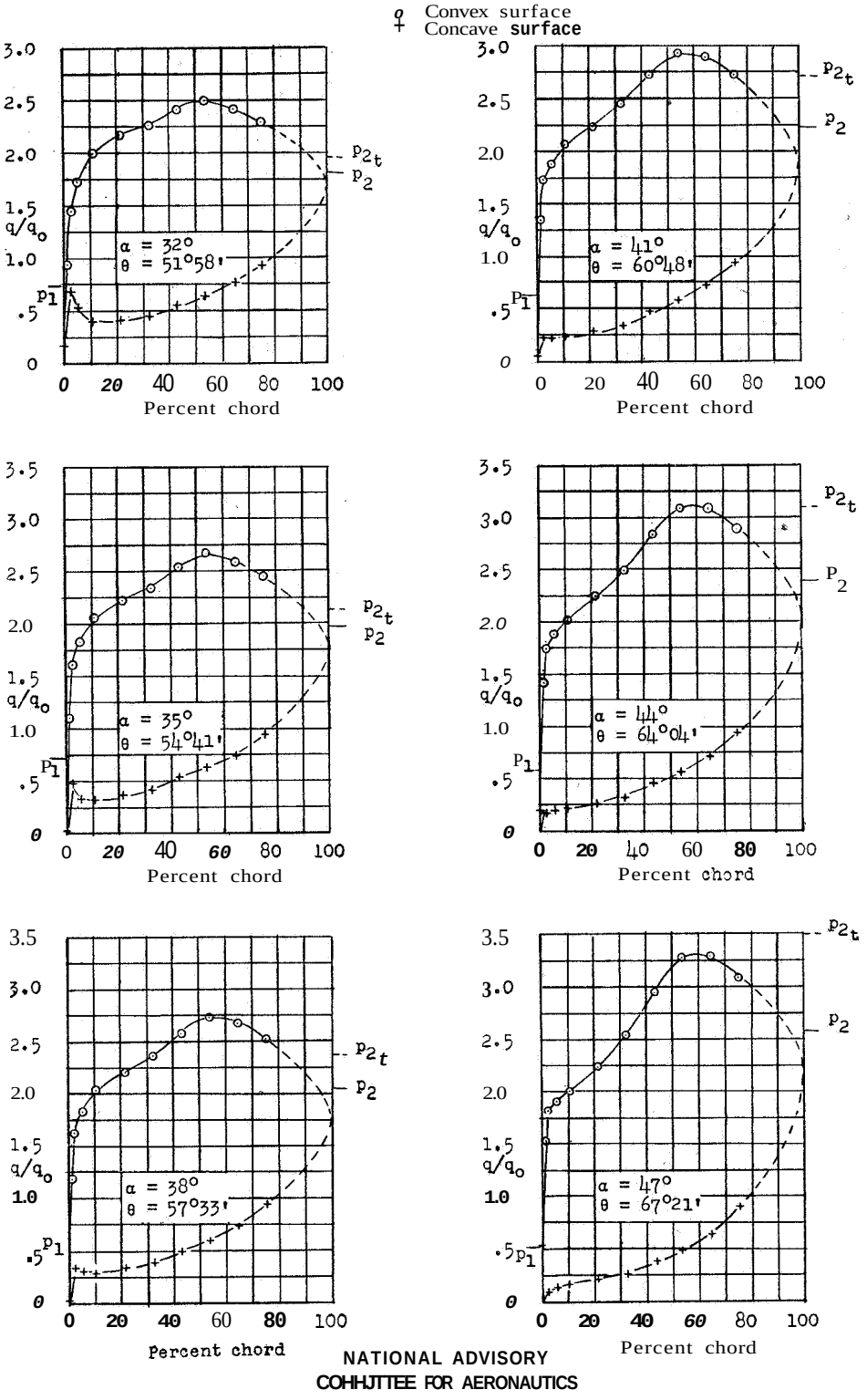

Figure 26.- Section pressure distributions for experimentally designed blower blade NACA 64-(C)06; stagger, 0°; solidity, 1.400; range of α_d, 32° to 44°.

o Convex surface
+ Concave surface

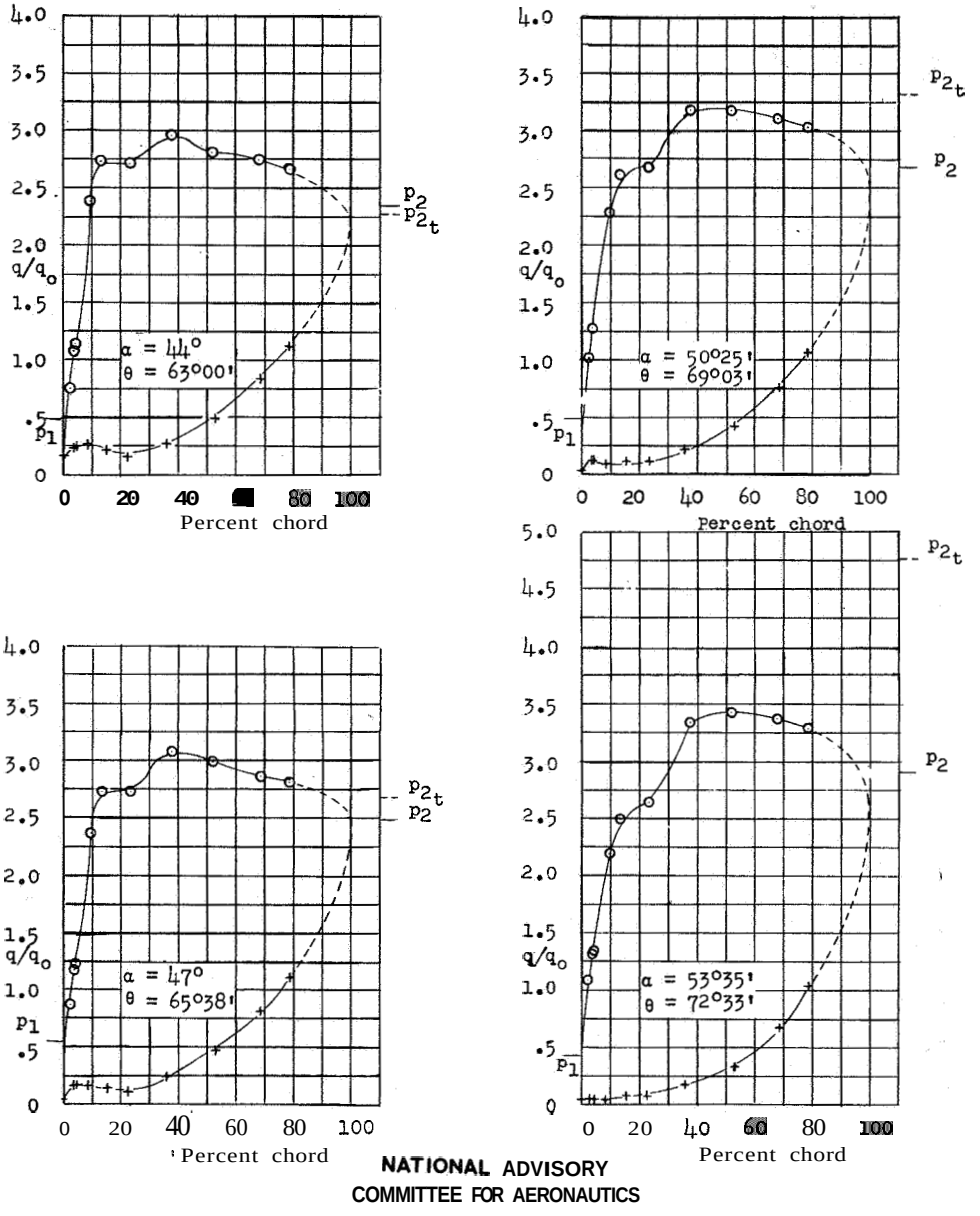

NATIONAL ADVISORY
COMMITTEE FOR AERONAUTICS

Figure 27.- Section pressure distributions for experimentally designed blower blade NACA 64-(D)06; stagger, 0°; solidity, 1.337; range of α_d, 44° to 61°.

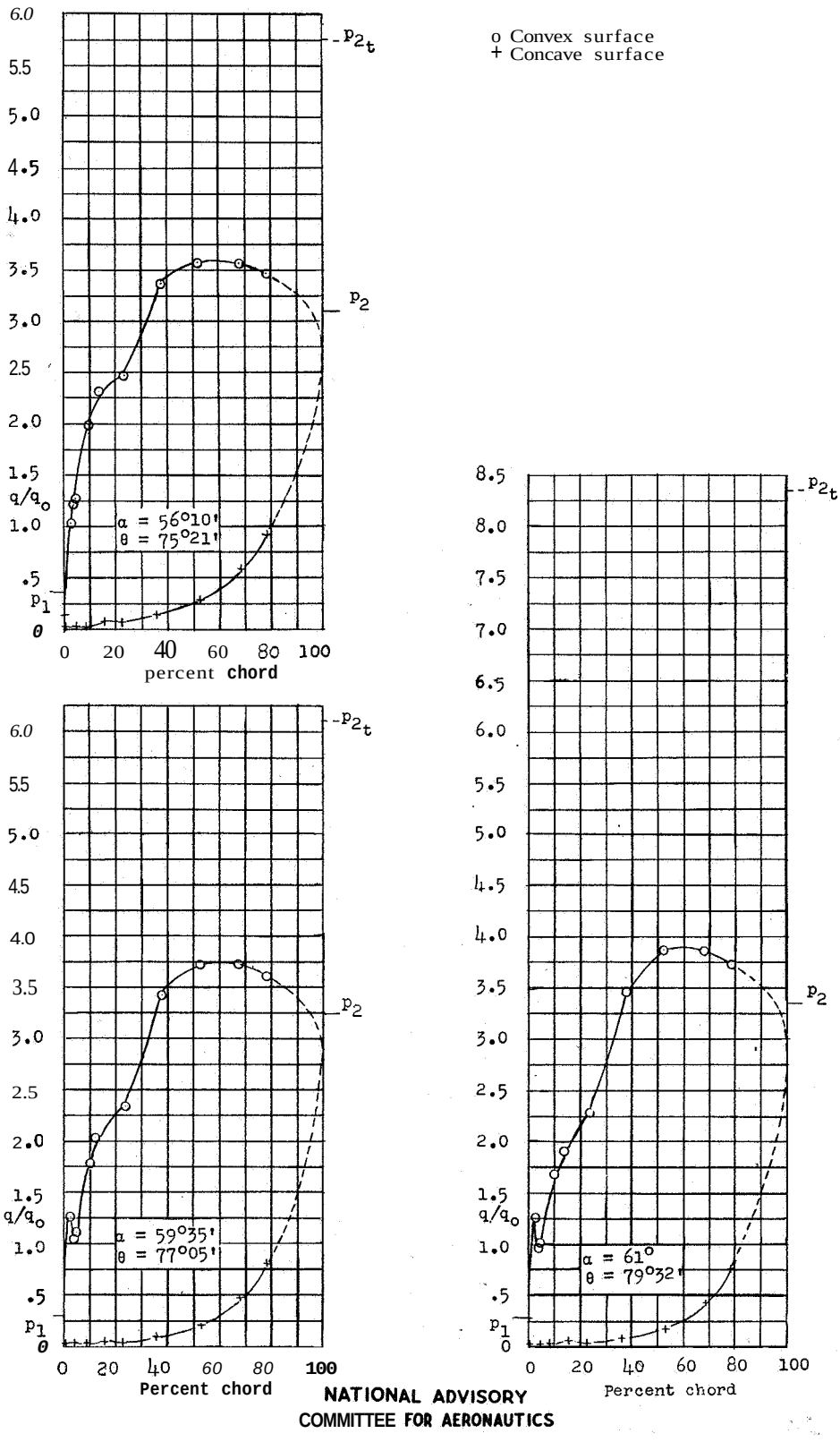

Figure 27.- Concluded.

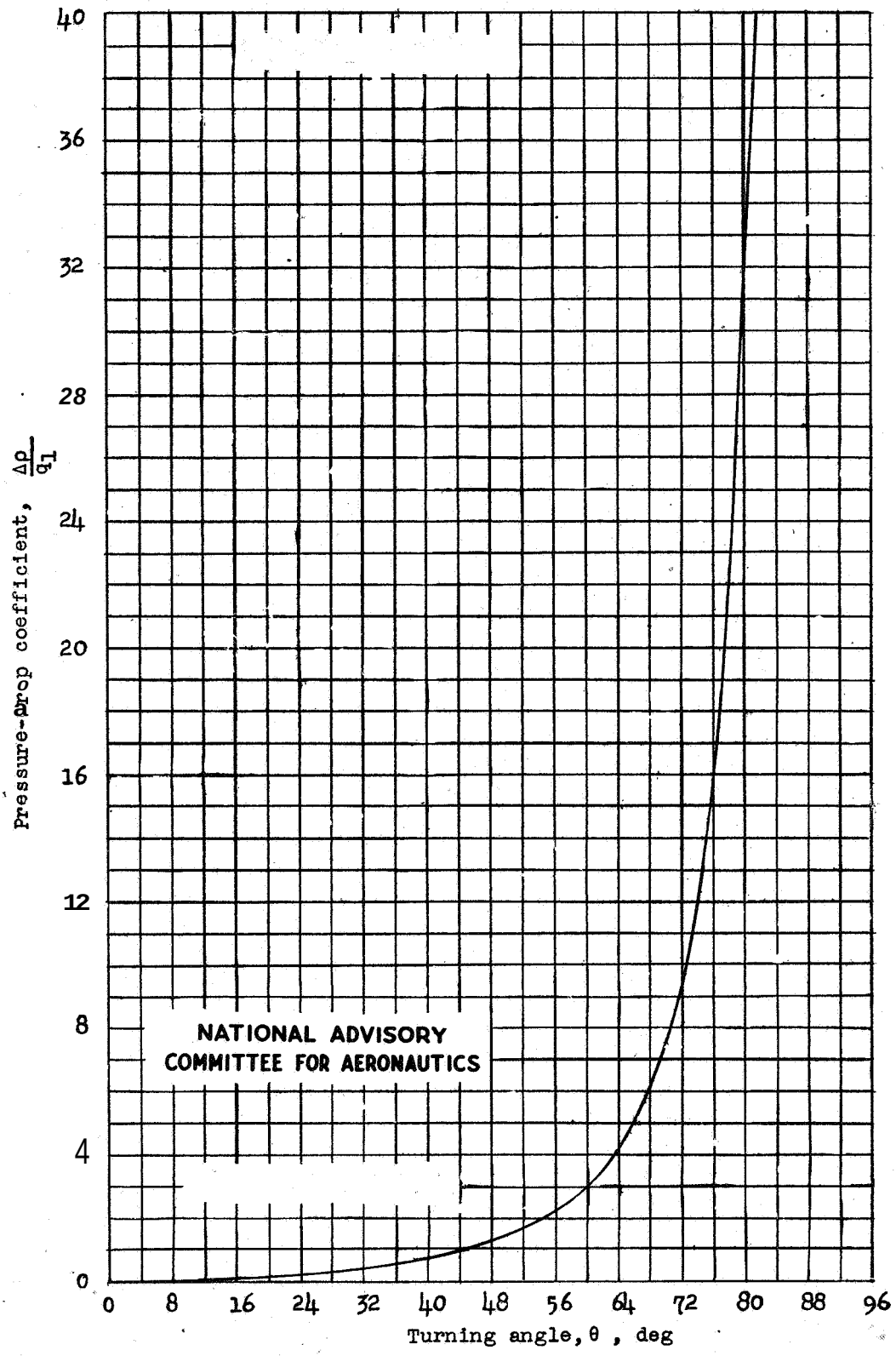

Figure 28.– Theoretical pressure drop through a cascade **at** 0° stagger.

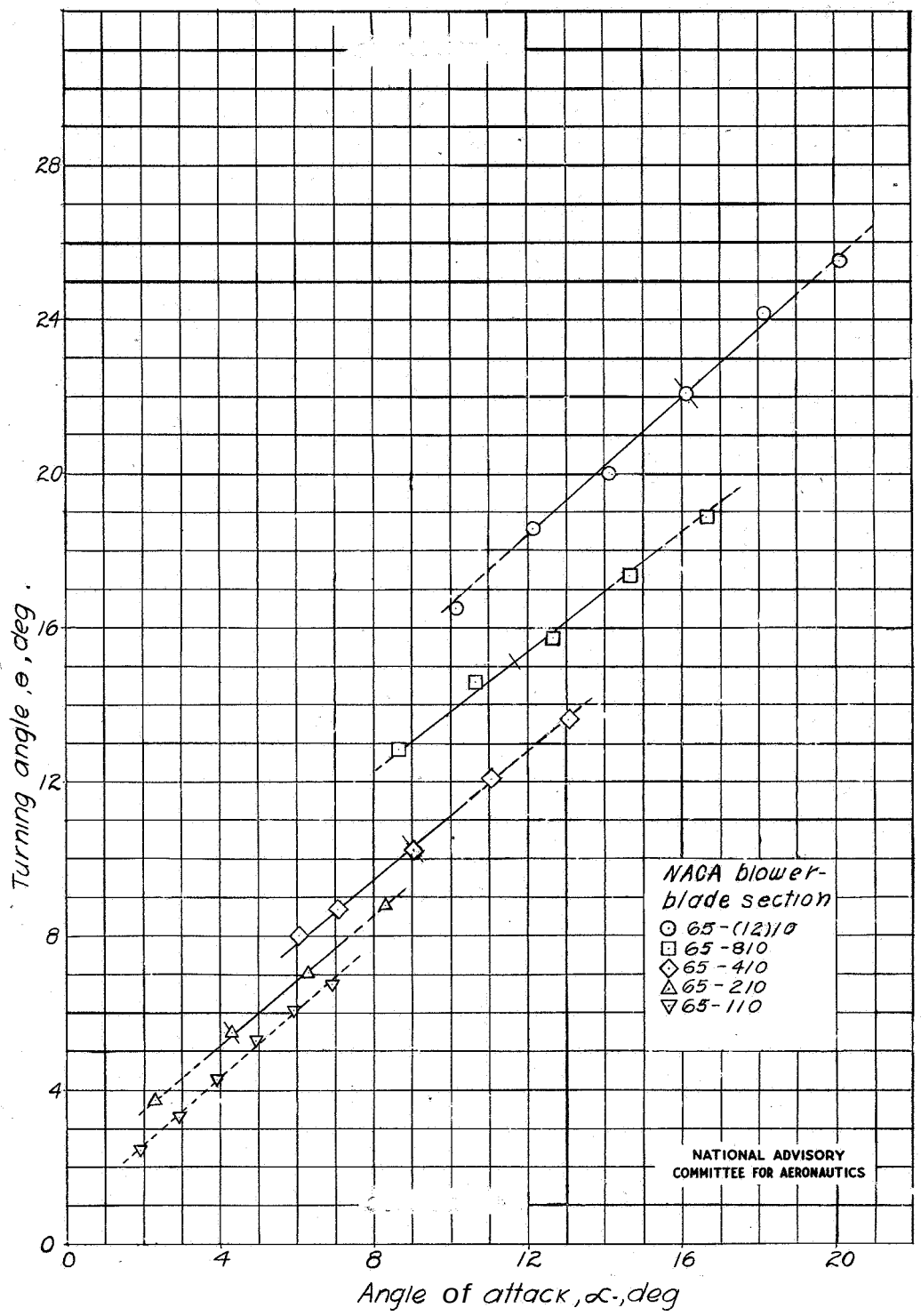

Figure 29.- Angle through which the air is turned in passing through a cascade. NACA 65-series blower-blade sections; stagger, 0°; solidity, 0.88. (Cross bar indicates design point; solid line indicates range of peak-free pressure distributions.)

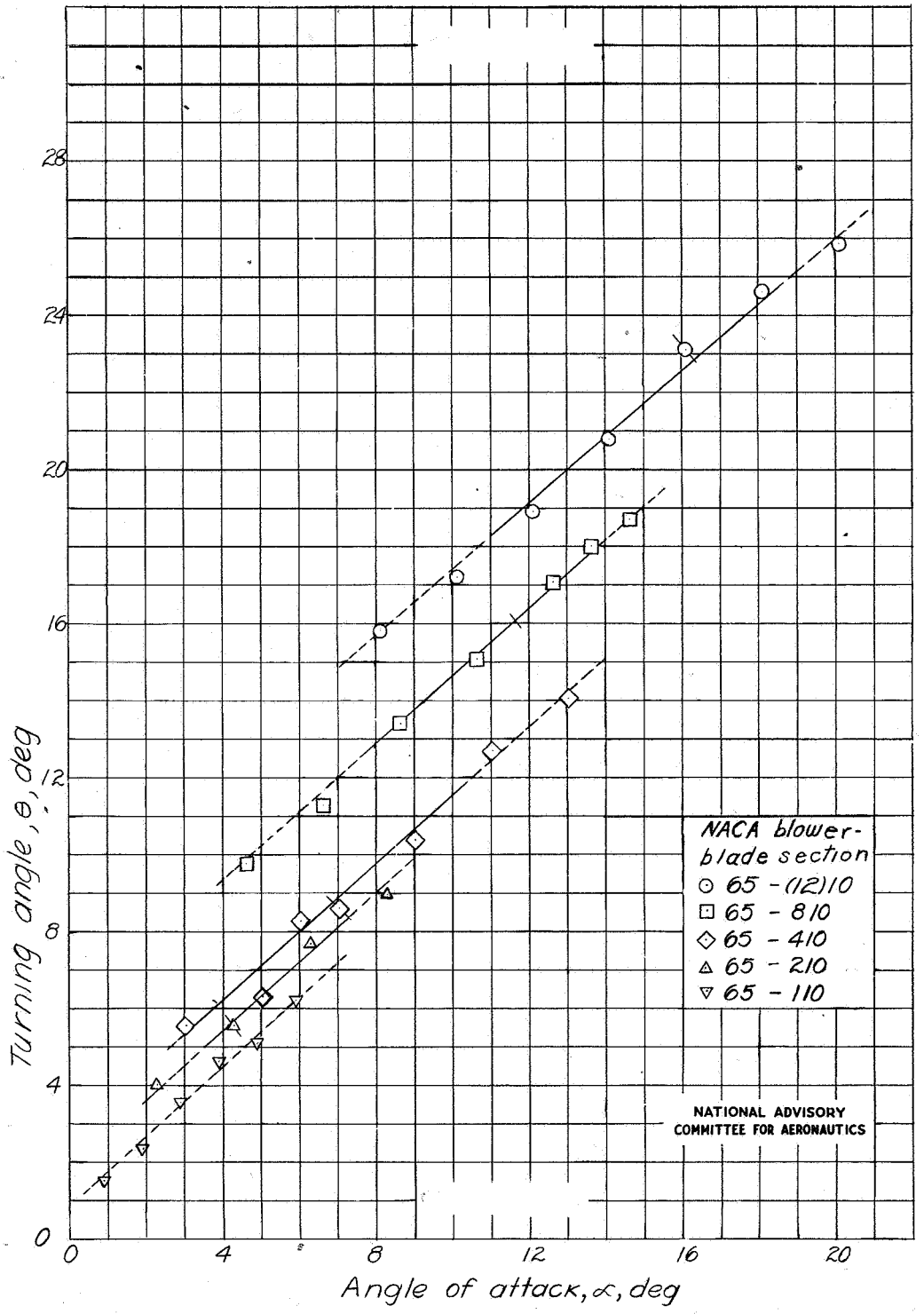

Figure 30.- Angle through which the air is turned in passing through a cascade. NACA 65-series blower-blade sections; stagger, 0°; solidity, 1.00. (Cross bar indicates design point; solid line indicates range of peak-free pressure distributions.)

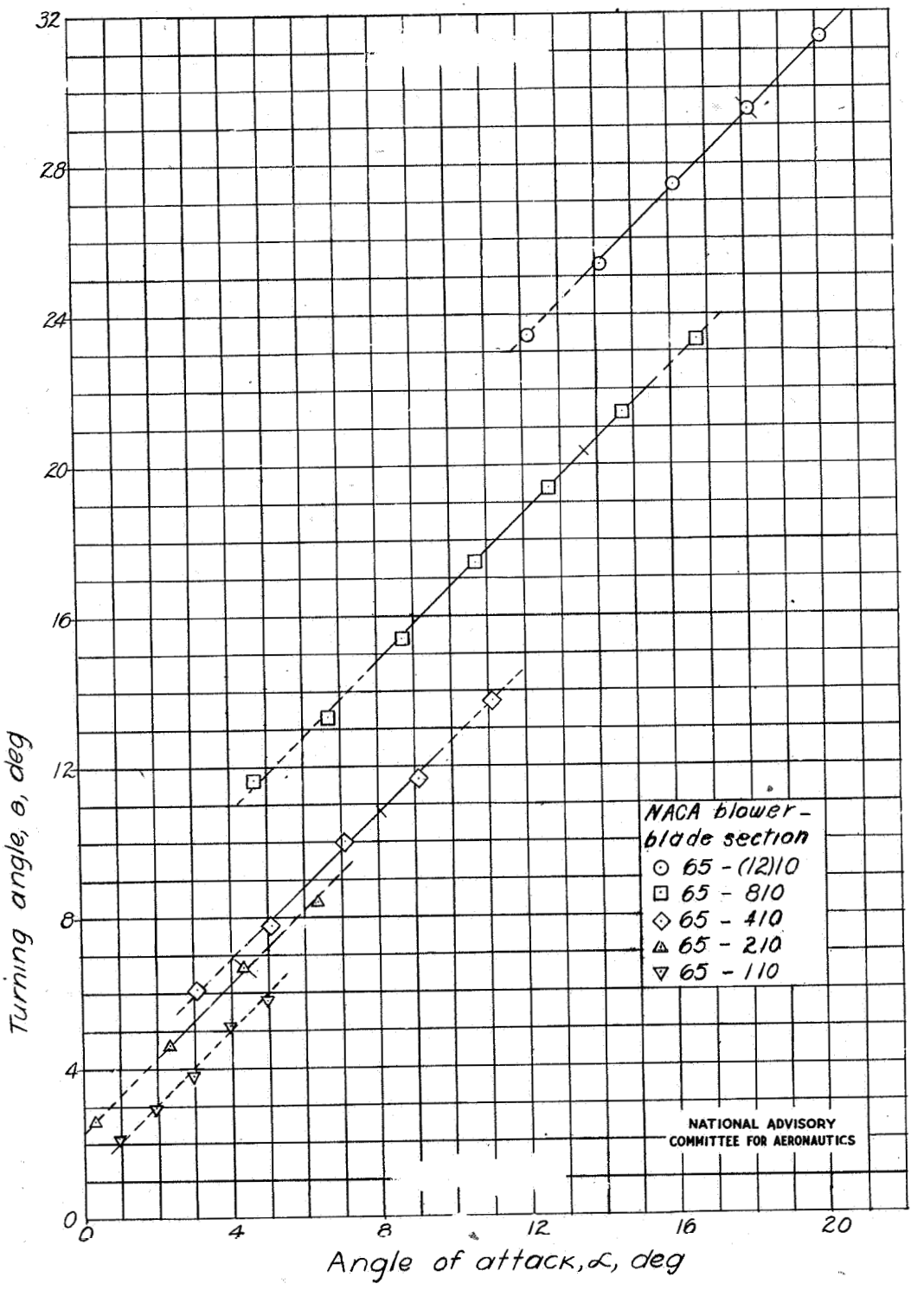

Figure 31.- Angle through which the air is turned in passing through a cascade. NACA 65-series blower-blade sections; stagger, 0°; solidity, 1.50. (Cross bar indicates design point; solid line indicates range of peak-free pressure distributions.)

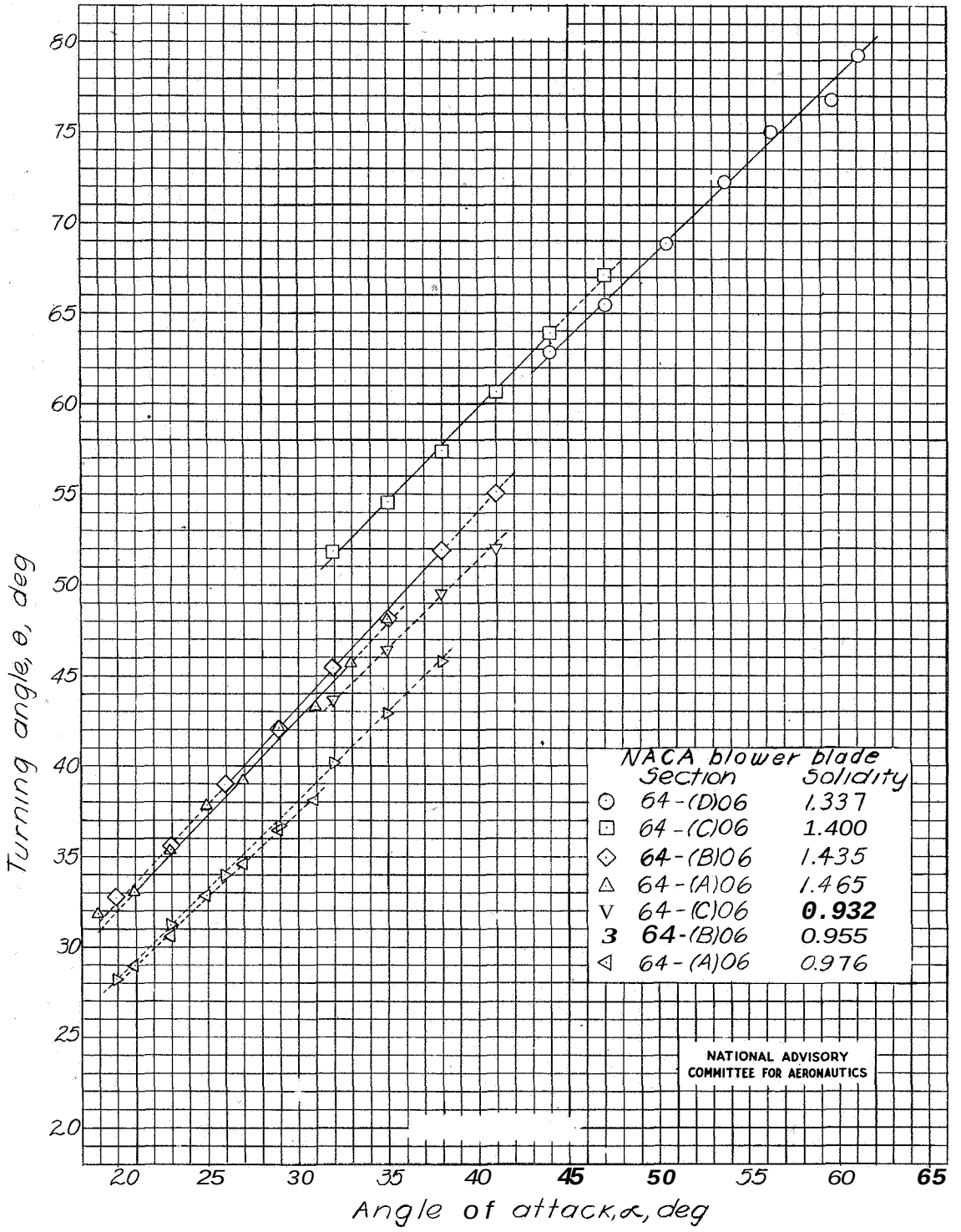

Figure 32.- Design chart of experimentally derived blower-blade sections at 0° stagger. (Solid lines indicate recommended turning angles.)

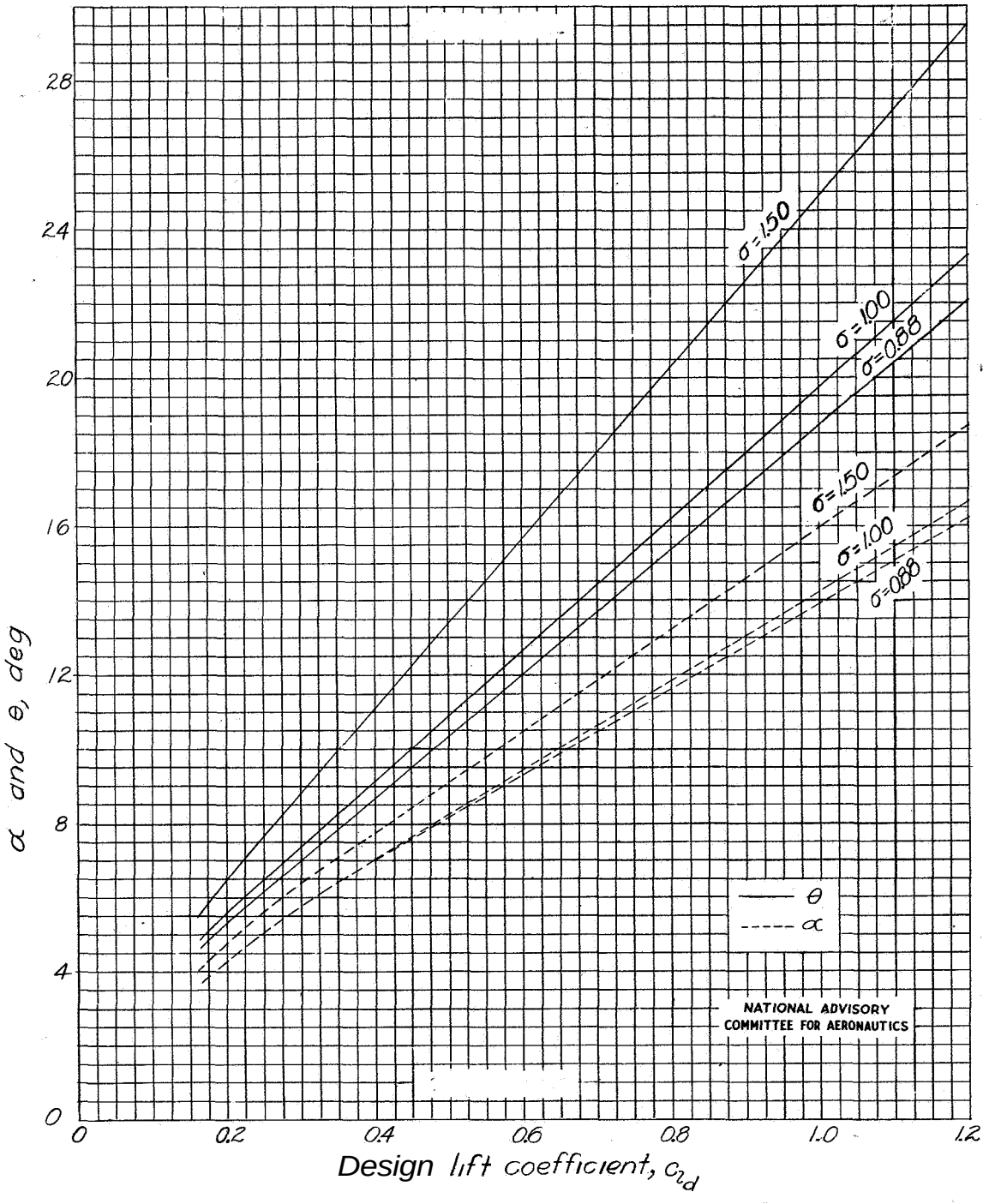

Figure 33.- Design chart for NACA 65-series blower-blade sections; stagger, 0°.